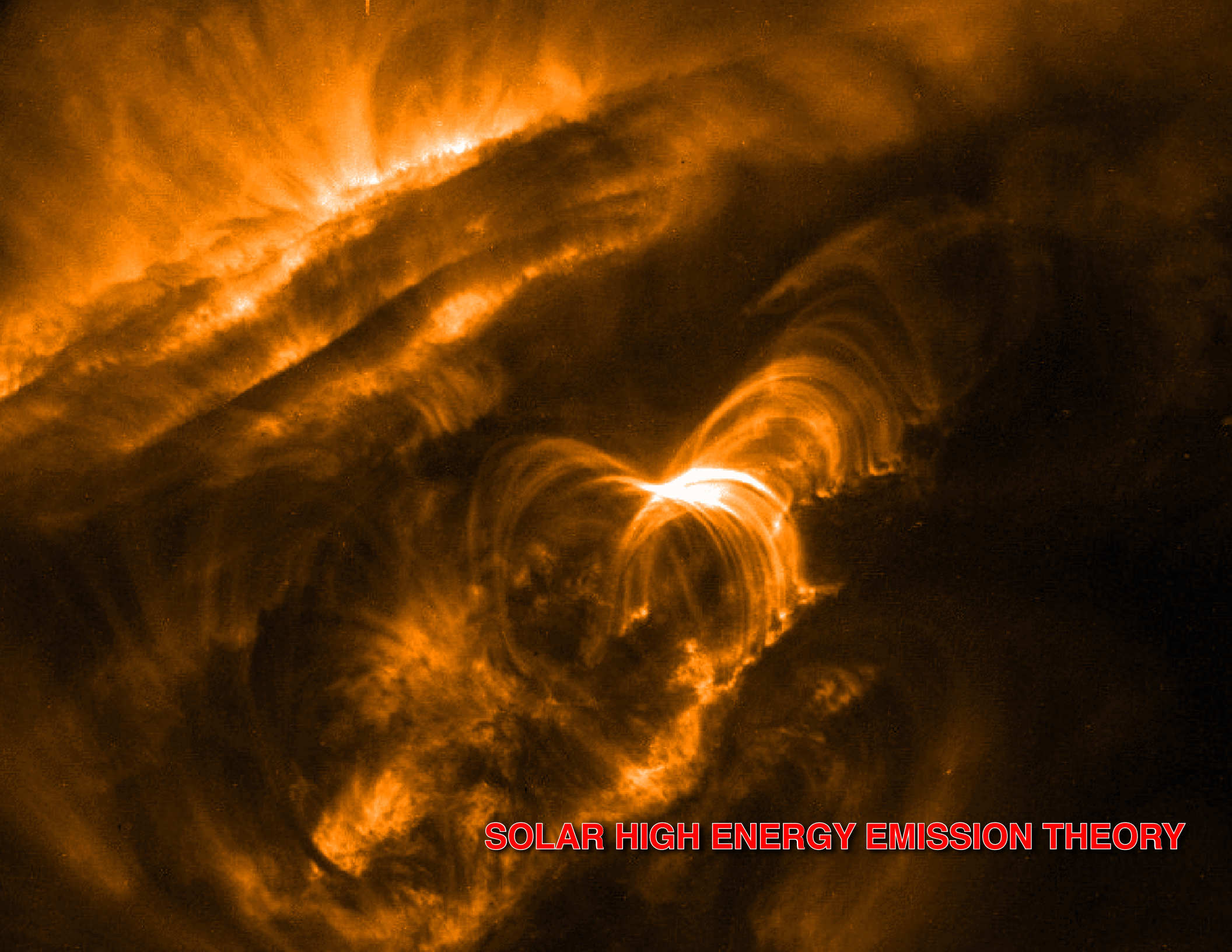

SOLAR HIGH ENERGY EMISSION THEORY

γ-ray and Neutron Production in Solar Flares

Yohkoh

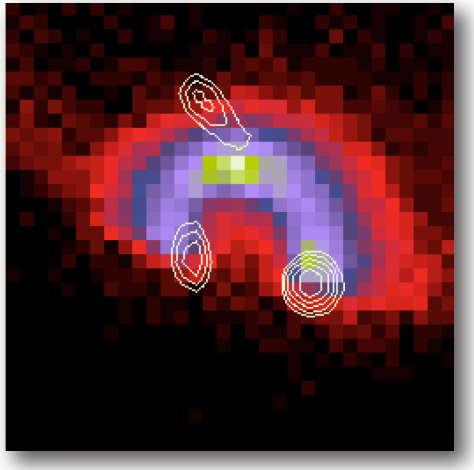

RHESSI

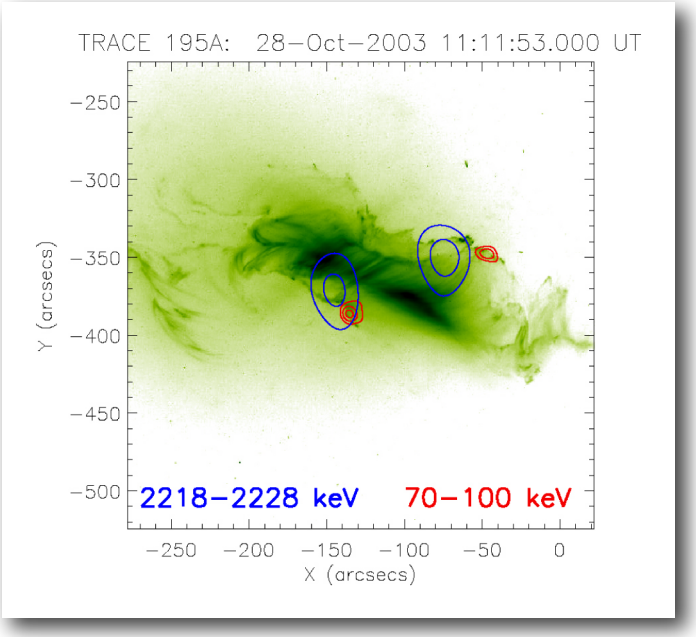

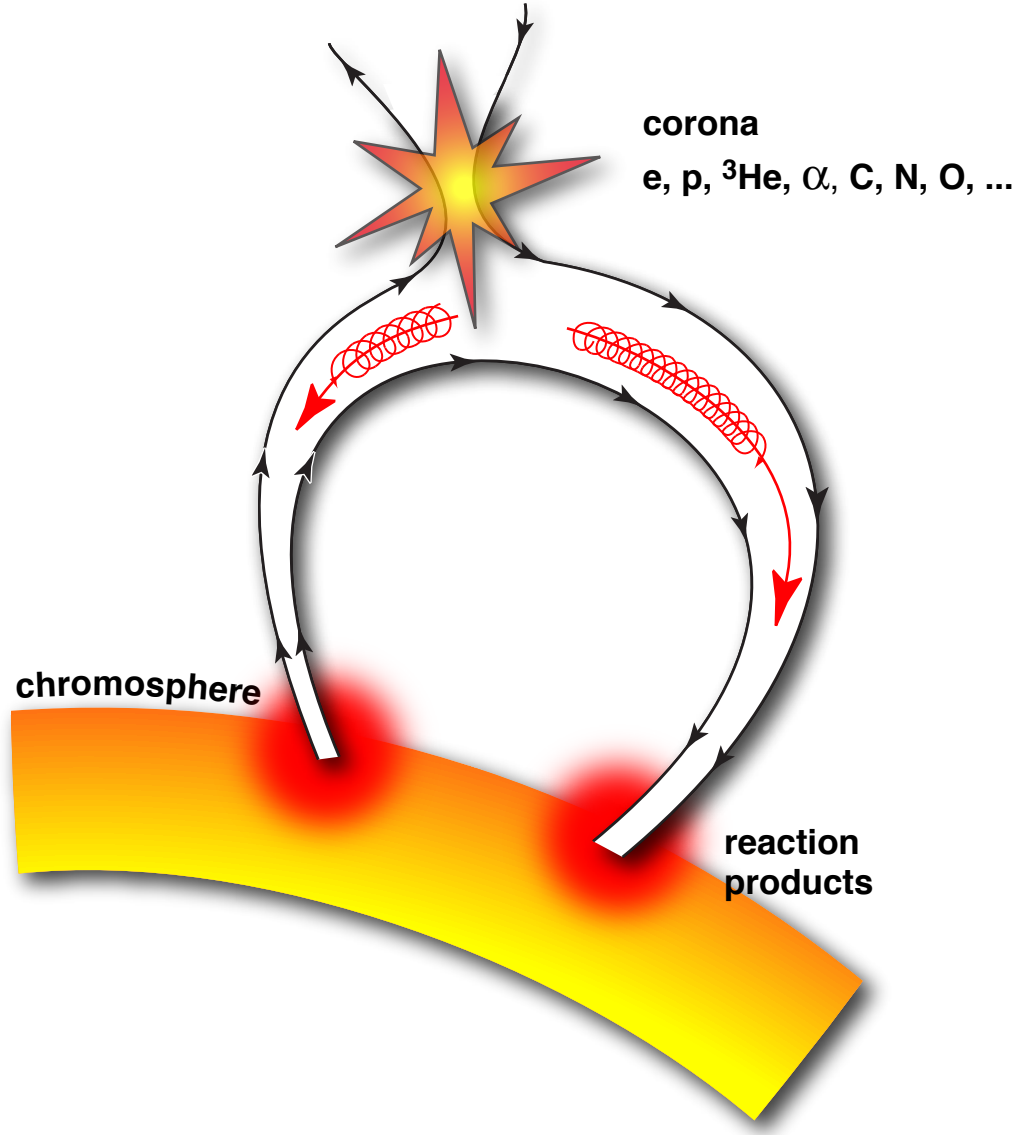

Products of Accelerated Particle Interactions

Products of interactions

e^-: X- and γ-ray bremsstrahlung

ions: excited nuclei

radioactive nuclei

neutrons

π^+, π^-, π^0

unlike atomic processes, nuclear reactions are not sensitive to the ambient environment temperature, density or charge state

Observable emission

excited nuclei $\rightarrow$ prompt γ-ray line radiation

radioactive nuclei $\rightarrow \begin{cases} \text{delayed } \gamma\text{-ray line radiation} \\ e^+ \rightarrow \gamma_{511} \text{ \& continuum} \end{cases}$

neutrons $\rightarrow \begin{cases} \text{escape into space} \\ \text{capture on H} \rightarrow d + \gamma_{2.223} \end{cases}$

$\pi \rightarrow \gamma$ (decay continuum, $e^\pm$ bremsstrahlung, γ_{511})

some of these observables are sensitive to the ambient environment temperature, density or charge state

Calculations of High-Energy Observable Emission

The traditional physics approach:

Develop a model for the flare process that can explain the observations with as few physically-based parameters as possible

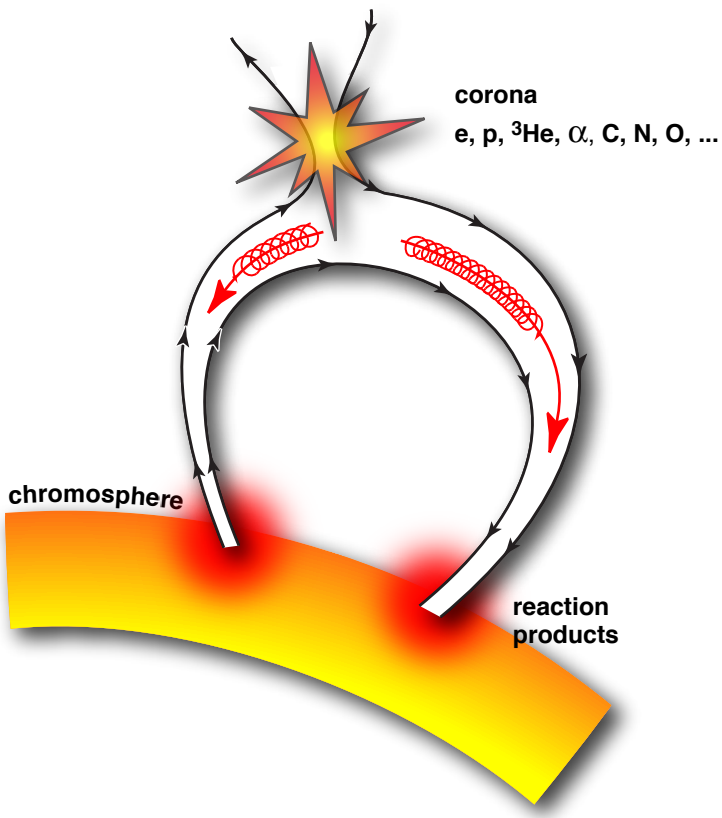

Transport and interaction model described by a set of parameters relating to conditions at the Sun,

$f(p_1, p_2, p_3, \ldots, p_n)$

↓

Predicted observable quantities

↓

Compare with measured observable quantities

↓

Modify parameters $p_1, p_2, p_3, \ldots, p_n$

Yield calculation

Thick target yield for a particular nuclear reaction from an ion with energy E_0 (MeV nucleon^{-1}):

cross section for the reaction

$$Q(E_0) = n\int_0^{E_0} dE \frac{\sigma(E)}{dE/dl(E)} P(E_0, E)$$

energy loss rate due to Coulomb interactions

total nuclear cross section

probability for removal by other nuclear reactions

$$P(E_0, E) = exp\left[-n\int_E^{E_0} \frac{\sigma_N(E')}{dE/dl(E')} dE'\right]$$

Thick target yield from a distribution of ions with an initial-energy spectrum $dN(E_0)/dE$ (MeV nucleon^{-1})$^{-1}$:

$$Q = \int_0^{\infty} dE_0 \frac{dN}{dE}(E_0)\, Q(E_0) = n\int_0^{\infty} dE_0 \frac{dN}{dE}(E_0) \int_0^{E_0} dE \frac{\sigma(E)}{dE/dl(E)} P(E_0, E)$$

Reaction Cross Section

Cross section differential in secondary energy E_s and secondary direction

$$\frac{d\sigma(E_0)}{dE_s\, d\Omega_s}$$

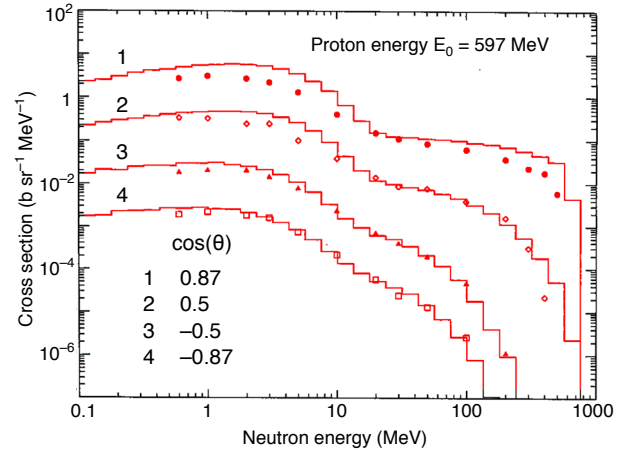

Cross section differential in secondary energy E_s

$$\frac{d\sigma(E_0)}{dE_s}$$

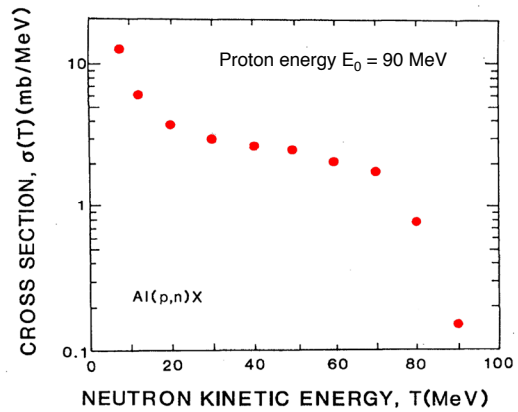

Total cross section

$$\sigma(E_0)$$

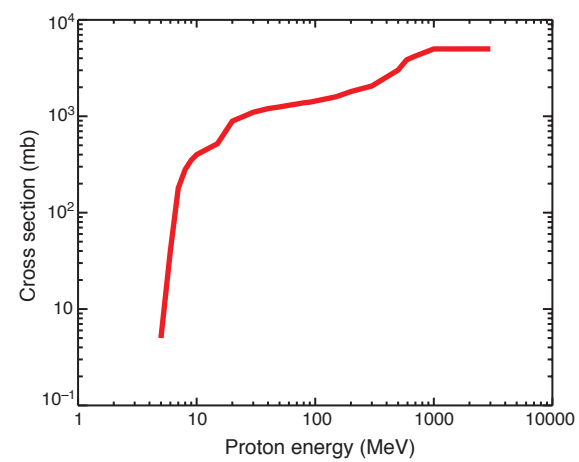

1 barn = 10^{-24} cm^2

Evaluation of Nuclear Reaction Cross Sections

CHALLENGE: Ions in solar flares are accelerated over a very broad range of energies, from <1 MeV nucleon^{-1} to more than a GeV nucleon^{-1}

- Cross section measurements are obtained from accelerator experiments
- No one accelerator covers the entire energy range; each covers only a fraction of the full range
- Some energy ranges are not covered at all
- Cannot rely solely on measurements

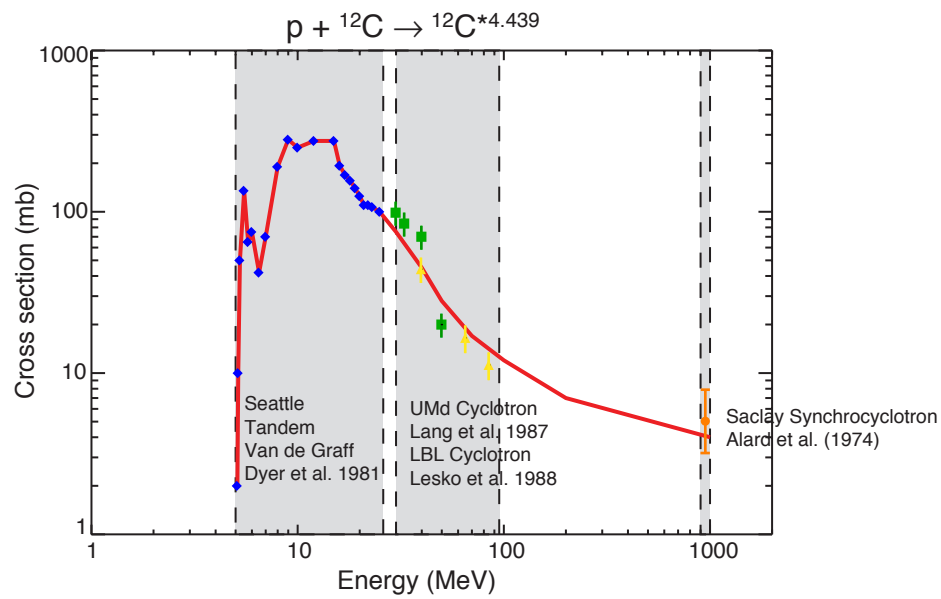

Evaluation of Nuclear Reaction Cross Sections (cont.)

SOLUTION: Need to include theoretical evaluations of cross sections to extend the energy coverage

- Nuclear physics theory

  nuclear reaction codes (e.g., EMPIRE, TALYS) use different calculation schemes for different targets and energy ranges

  e.g., heavy target/low energy → 2-stage interaction through "compound nucleus"

  high energy → 2-body nucleon-nucleon interaction

- Empirical rules

  e.g., 2-particle product at high energy → exponential decay at high energy

  multi-particle product (spallation) → plateau at high energy

  similar reaction & similar target should exhibit similar energy dependence

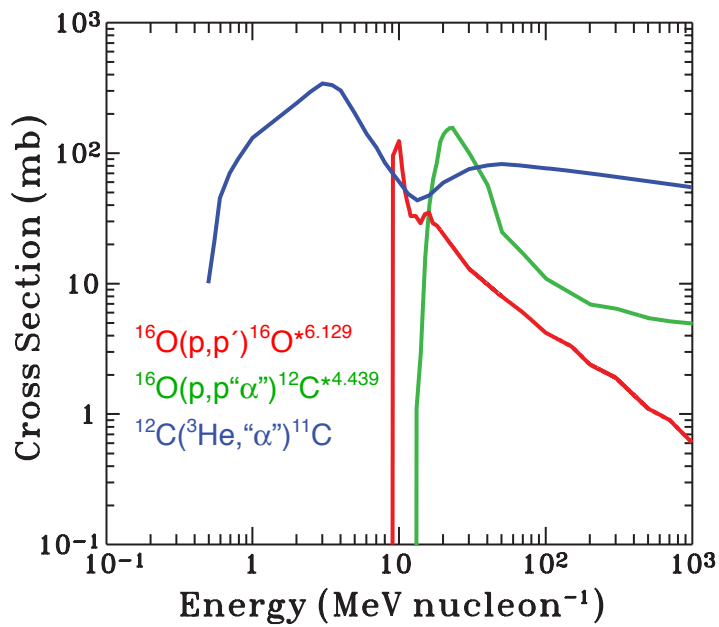

Evaluation of Nuclear Reaction Cross Sections (cont.)

Final evaluated cross section is based on a combination of measurements, nuclear reaction theory, and empirical rules.

Improvements in our knowledge of the cross sections have been a continuous process since the 1980s.

Improvements in measurements of solar flares continue to demand further improvements.

Deexcitation Lines
Ramaty, Kozlovsky & Lingenfelter 1979, ApJS, 40, 487
Kozlovsky, Murphy & Ramaty 2002, ApJS, 141, 523
Tatischeff, Kozlovsky, Kiener & Murphy, 2006, ApJ, in press

Positrons
Kozlovsky, Lingenfleter & Ramaty 1987, ApJ, 316, 801
Kozlovsky, Murphy & Share 2004, ApJ, 604, 892

Neutrons
Hua, Kozlovsky, Lingenfelter, Ramaty & Stupp, 2002, ApJS, 140, 563

High Energy Observable Emission

nuclear deexcitation gamma-ray lines

positron annihilation line

escaping neutrons

neutron capture line

pion decay emission

Nuclear Deexcitation Gamma-Ray Lines

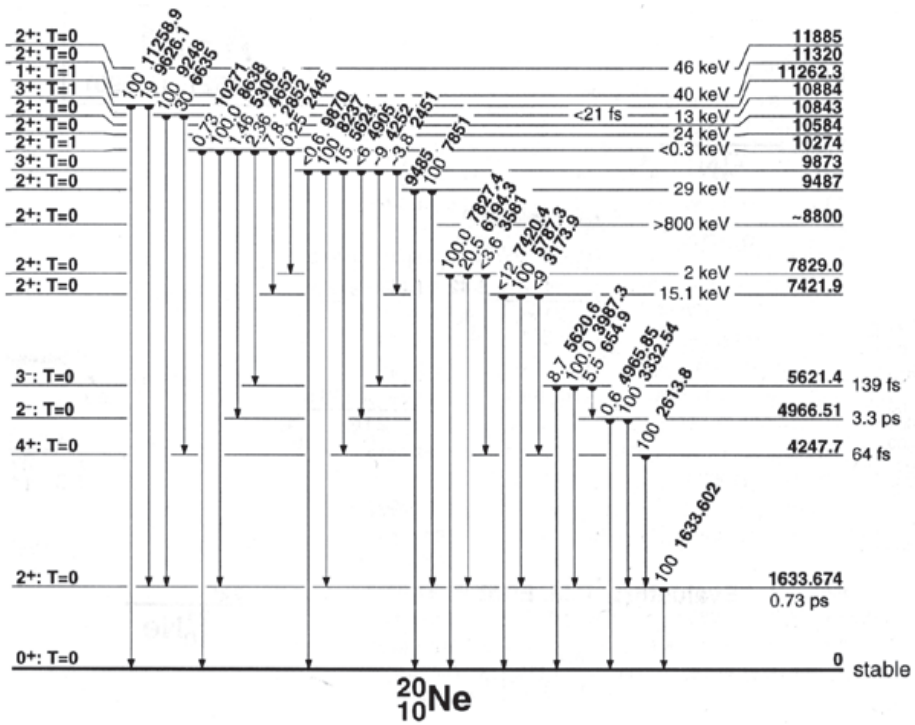

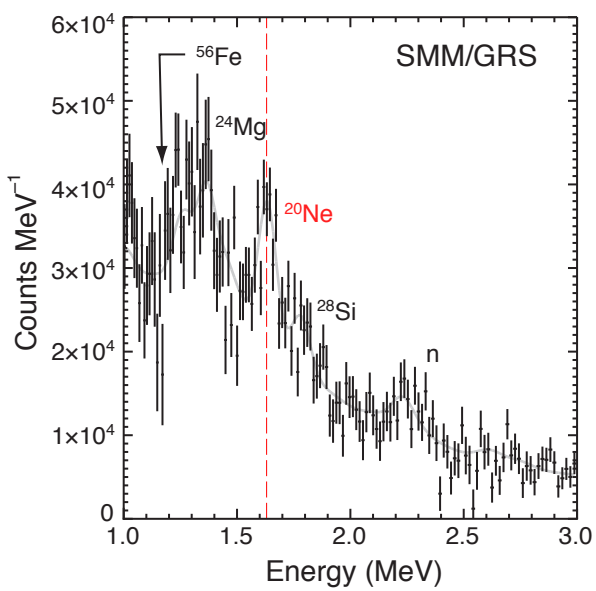

INELASTIC direct

$$\left.\begin{matrix} p \\ \alpha \end{matrix}\right\} + {}^{20}Ne \longrightarrow {}^{20}Ne^{*1.634}$$

INELASTIC inverse

$${}^{20}Ne + \left\{\begin{matrix} H \\ He \end{matrix}\right. \longrightarrow {}^{20}Ne^{*1.634}$$

SPALLATION direct

$$\left.\begin{matrix} p \\ \alpha \end{matrix}\right\} + {}^{24}Mg \longrightarrow {}^{20}Ne^{*1.634} + \ldots$$

SPALLATION inverse

$${}^{24}Mg + \left\{\begin{matrix} H \\ He \end{matrix}\right. \longrightarrow {}^{20}Ne^{*1.634} + \ldots$$

FUSION

$$\cancel{\alpha + {}^{16}O \longrightarrow {}^{20}Ne^{*1.634} + \gamma}$$

$${}^{3}He + {}^{16}O \longrightarrow {}^{18}F^{*1.040} + p$$

$$\alpha + {}^{4}He \longrightarrow {}^{7}Be^{*0.429} + n$$

$$\alpha + {}^{4}He \longrightarrow {}^{7}Li^{*0.478} + p$$

Nuclear Deexcitation Gamma-Ray Lines (cont.)

Energy (MeV)	Reaction
0.092	$^{55}Fe^{*1.408} \rightarrow {}^{55}Fe^{*1.317}$
0.110	$^{19}F^{*0.110} \rightarrow$g.s.
0.158	$^{56}Co^{*0.158} \rightarrow$g.s.
0.197	$^{19}F^{*0.197} \rightarrow$g.s.
0.238	$^{19}Ne^{*0.238} \rightarrow$g.s.
0.275	$^{19}Ne^{*0.275} \rightarrow$g.s.
0.339	$^{59}Ni^{*0.339} \rightarrow$g.s.
0.411	$^{55}Fe^{*0.411} \rightarrow$g.s.
0.429	$^{7}Be^{*0.429} \rightarrow$g.s.
0.440	$^{23}Na^{*0.440} \rightarrow$g.s.
0.451	$^{23}Mg^{*0.451} \rightarrow$g.s.
0.477	$^{55}Fe^{*1.408} \rightarrow {}^{55}Fe^{*0.931}$
0.478	$^{7}Li^{*0.478} \rightarrow$g.s.
0.718	$^{10}B^{*0.718} \rightarrow$g.s.
0.744	$^{52}Cr^{*3.114} \rightarrow {}^{52}Cr^{*2.370}$
0.781	$^{27}Si^{*0.781} \rightarrow$g.s.
0.812	$^{56}Co^{*0.970} \rightarrow {}^{56}Co^{*0.158}$
0.835	$^{54}Cr^{*0.835} \rightarrow$g.s.
0.844	$^{27}Al^{*0.844} \rightarrow$g.s.
0.847	$^{56}Fe^{*0.847} \rightarrow$g.s.
0.891	$^{22}Na^{*0.891} \rightarrow$g.s.
0.931	$^{55}Fe^{*0.931} \rightarrow$g.s.
0.936	$^{52}Cr^{*2.370} \rightarrow {}^{52}Cr^{*1.434}$
0.937	$^{18}F^{*0.937} \rightarrow$g.s.
0.957	$^{27}Si^{*0.957} \rightarrow$g.s.
0.984	$^{48}Ti^{*0.984} \rightarrow$g.s.
0.999	$^{59}Ni^{*1.338} \rightarrow {}^{59}Ni^{*0.339}$
1.005	$^{58}Ni^{*2.459} \rightarrow {}^{58}Ni^{*1.454}$
1.014	$^{27}Al^{*1.014} \rightarrow$g.s.
1.022	$^{10}B^{*1.740} \rightarrow {}^{10}B^{*0.718}$
1.038	$^{56}Fe^{*3.123} \rightarrow {}^{56}Fe^{*2.085}$
1.042	$^{18}F^{*1.042} \rightarrow$g.s.
1.049	$^{58}Co^{*1.049} \rightarrow$g.s.
1.081	$^{18}F^{*1.081} \rightarrow$g.s.
1.130	$^{54}Fe^{*2.538} \rightarrow {}^{54}Fe^{*1.408}$

Energy (MeV)	Reaction
1.189	$^{59}Ni^{*1.189} \rightarrow$g.s.
1.190	$^{59}Co^{*1.190} \rightarrow$g.s.
1.223	$^{55}Fe^{*2.539} \rightarrow {}^{55}Fe^{*1.317}$
1.238	$^{56}Fe^{*2.085} \rightarrow {}^{56}Fe^{*0.847}$
1.249	$^{31}S^{*1.249} \rightarrow$g.s.
1.266	$^{31}P^{*1.266} \rightarrow$g.s.
1.275	$^{22}Ne^{*1.275} \rightarrow$g.s.
1.312	$^{48}Ti^{*2.296} \rightarrow {}^{48}Ti^{*0.984}$
1.317	$^{55}Fe^{*1.317} \rightarrow$g.s.
1.334	$^{52}Cr^{*2.768} \rightarrow {}^{52}Cr^{*1.434}$
1.367	$^{59}Ni^{*2.705} \rightarrow {}^{59}Ni^{*1.338}$
1.369	$^{24}Mg^{*1.369} \rightarrow$g.s.
1.370	$^{55}Fe^{*2.301} \rightarrow {}^{55}Fe^{*0.931}$
1.408	$^{55}Fe^{*1.408} \rightarrow$g.s.
1.428	$^{59}Ni^{*1.767} \rightarrow {}^{59}Ni^{*0.339}$
1.434	$^{52}Cr^{*1.434} \rightarrow$g.s.
1.441	$^{53}Mn^{*1.441} \rightarrow$g.s.
1.454	$^{58}Ni^{*1.454} \rightarrow$g.s.
1.460	$^{59}Co^{*1.460} \rightarrow$g.s.
1.600	$^{23}Mg^{*2.051} \rightarrow {}^{23}Mg^{*0.451}$
1.635	$^{14}N^{*3.948} \rightarrow {}^{14}N^{*2.313}$
1.634	$^{20}Ne^{*1.634} \rightarrow$g.s.
1.636	$^{23}Na^{*2.076} \rightarrow {}^{23}Na^{*0.440}$
1.771	$^{56}Fe^{*3.856} \rightarrow {}^{56}Fe^{*2.085}$
1.779	$^{28}Si^{*1.779} \rightarrow$g.s.
1.809	$^{26}Mg^{*1.809} \rightarrow$g.s.
1.811	$^{56}Fe^{*2.658} \rightarrow {}^{56}Fe^{*0.847}$
2.000	$^{11}C^{*2.000} \rightarrow$g.s.
2.029	$^{31}P^{*3.295} \rightarrow {}^{31}P^{*1.266}$
2.034	$^{31}S^{*3.283} \rightarrow {}^{31}S^{*1.249}$
2.094	$^{56}Fe^{*2.942} \rightarrow {}^{56}Fe^{*0.847}$
2.113	$^{56}Fe^{*2.960} \rightarrow {}^{56}Fe^{*0.847}$
2.124	$^{11}B^{*2.125} \rightarrow$g.s.
2.164	$^{27}Si^{2.164} \rightarrow$g.s.
2.211	$^{27}Al^{*2.211} \rightarrow$g.s.

Energy (MeV)	Reaction
2.230	$^{32}S^{*2.230} \rightarrow$g.s.
2.232	$^{31}S^{*2.232} \rightarrow$g.s.
2.234	$^{31}P^{*2.234} \rightarrow$g.s.
2.263	$^{23}Na^{*2.704} \rightarrow {}^{23}Na^{*0.440}$
2.313	$^{14}N^{*2.313} \rightarrow$g.s.
2.598	$^{56}Fe^{*3.449} \rightarrow {}^{56}Fe^{*0.847}$
2.614	$^{20}Ne^{*4.248} \rightarrow {}^{20}Ne^{*1.634}$
2.640	$^{23}Na^{*2.640} \rightarrow$g.s.
2.742	$^{16}O^{*8.872} \rightarrow {}^{16}O^{*6.130}$
2.754	$^{24}Mg^{*4.123} \rightarrow {}^{24}Mg^{*1.369}$
3.333	$^{20}Ne^{*4.967} \rightarrow {}^{20}Ne^{*1.634}$
3.562	$^{6}Li^{*3.563} \rightarrow$g.s.
3.684	$^{13}C^{*3.685} \rightarrow$g.s.
3.736	$^{40}Ca^{*3.736} \rightarrow$g.s.
3.853	$^{13}C^{*3.854} \rightarrow$g.s.
4.438	$^{12}C^{*4.439} \rightarrow$g.s.
4.444	$^{11}B^{*4.445} \rightarrow$g.s.
5.099	$^{28}Si^{*6.879} \rightarrow {}^{28}Si^{*1.779}$
5.105	$^{14}N^{*5.106} \rightarrow$g.s.
5.180	$^{15}O^{5.181} \rightarrow$g.s.
5.240	$^{15}O^{*5.241} \rightarrow$g.s.
5.269	$^{15}N^{*5.270} \rightarrow$g.s.
5.298	$^{15}N^{*5.299} \rightarrow$.g.s.
6.129	$^{16}O^{*6.130} \rightarrow$g.s.
6.175	$^{15}O^{*6.176} \rightarrow$g.s.
6.322	$^{15}N^{*6.324} \rightarrow$g.s.
6.337	$^{11}C^{*6.339} \rightarrow$g.s.
6.476	$^{11}C^{*6.478} \rightarrow$g.s.
6.741	$^{11}B^{*6.743} \rightarrow$g.s.
6.790	$^{11}B^{*6.792} \rightarrow$g.s.
6.879	$^{28}Si^{*6.879} \rightarrow$g.s.
6.916	$^{16}O^{*6.917} \rightarrow$g.s.
7.115	$^{16}O^{*7.117} \rightarrow$g.s.
7.299	$^{15}N^{*7.301} \rightarrow$g.s.
15.10	$^{12}C^{*15.11} \rightarrow$g.s.

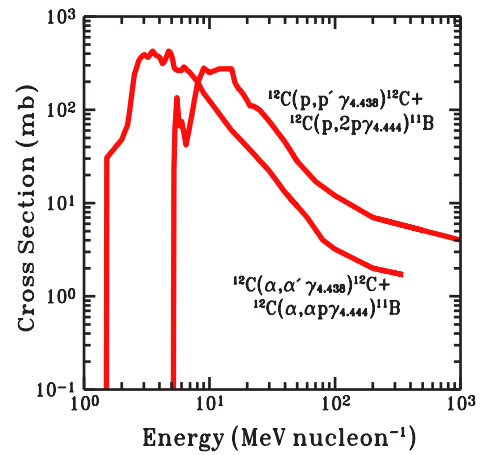

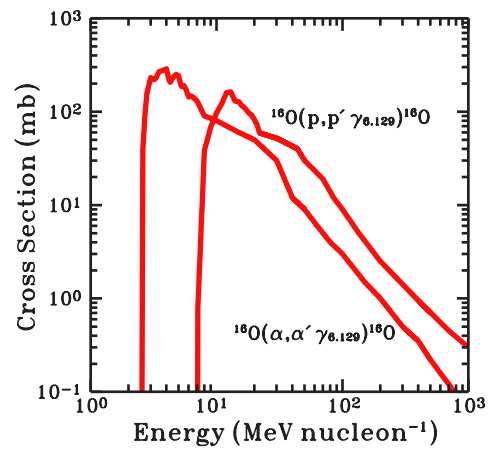

Measured cross sections to produce the lines obtained from high-quality laboratory measurements by Dyer, Bodansky, Lang, Kiener, Tatischeff, etc.

Nuclear Deexcitation Gamma-Ray Lines (cont.)
Prompt vs.Delayed Emission

Prompt

Excited nuclei deexcite quickly.

Nucleus	Mean lifetime τ (s)
$^{20}Ne^{*1.634}$	1.2×10^{-12}
$^{12}C^{*4.439}$	5.6×10^{-14}
$^{16}O^{*6.129}$	2.4×10^{-11}

Delayed

Delayed decay of radioactive nuclei into daughter nuclei in an excited state. The daughter nuclei deexcite promptly

Reaction	Half-life $\tau_{1/2}$
$^{56}Fe(p,n)^{56}Co \xrightarrow[\tau_{1/2}]{} {}^{56}Fe^{*} \rightarrow {}^{56}Fe + \gamma_{0.847}$	77 days

Tatischeff, Kozlovsky, Kiener & Murphy 2006, ApJ, in press

Nuclear Deexcitation Gamma-Ray Lines (cont.)
Line Shapes

Gamma-ray is Doppler shifted due to velocity of emitting nucleus

$$\varepsilon' = \varepsilon \frac{(1 - \beta^2)^{1/2}}{(1 - \beta \cos\theta)}$$

$$\beta = v/c$$

Direct reaction

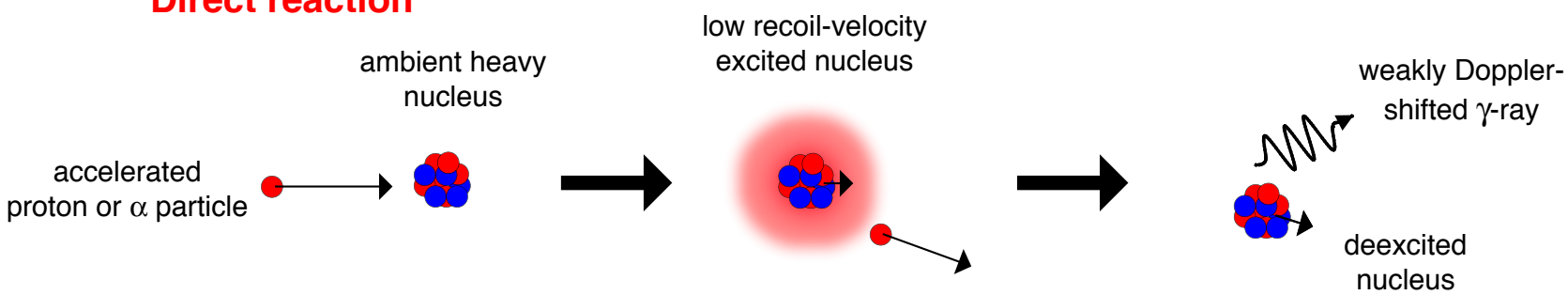

Inverse reaction

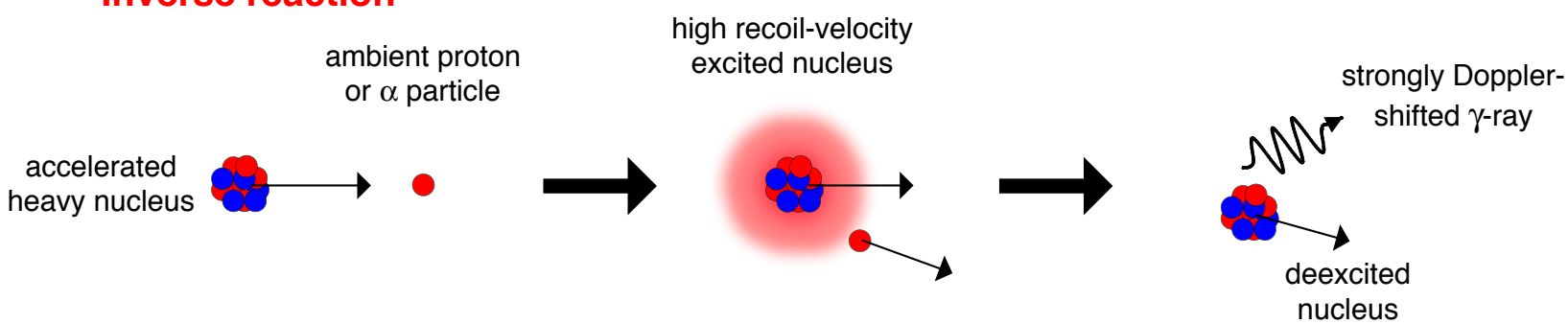

Nuclear Deexcitation Gamma-Ray Lines (cont.)
Line Shapes

Direct reaction → "narrow" line (FWHM 1 – 2%)
Inverse reaction → "broad" line (FWHM ~20%)

4.438 MeV ^{12}C line
Isotropic accelerated-particle angular distribution

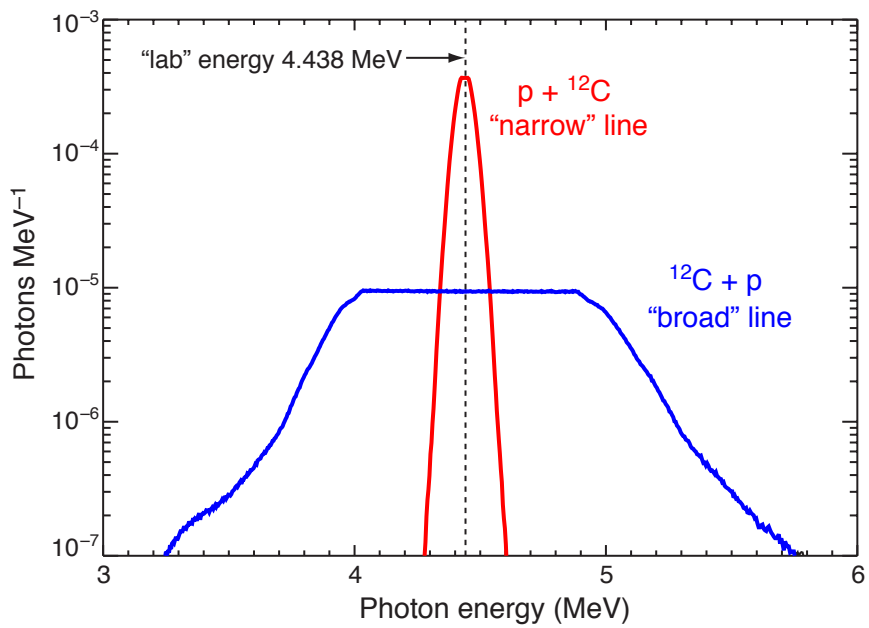

Note! This is true in a GAS where $\tau_{slow} > \tau_{life}$. The line width then reflects the recoil velocity and therefore retains information about the interaction.

But in the high density of a solid, τ_{slow} can be less than τ_{life}. The ^{16}O line from solids is very narrow while the ^{12}C line is not (τ_{life} of O is ~10^{-11} s but τ_{life} of C is ~10^{-14} s). This can be seen in laboratory measurements and is expected from grains in the ISM.

Nuclear Deexcitation Gamma-Ray Lines (cont.)
Line Shapes

Narrow line structure
Heavier α-particle produces more Doppler shift

4.438 MeV ^{12}C line
Isotropic accelerated-particle angular distribution

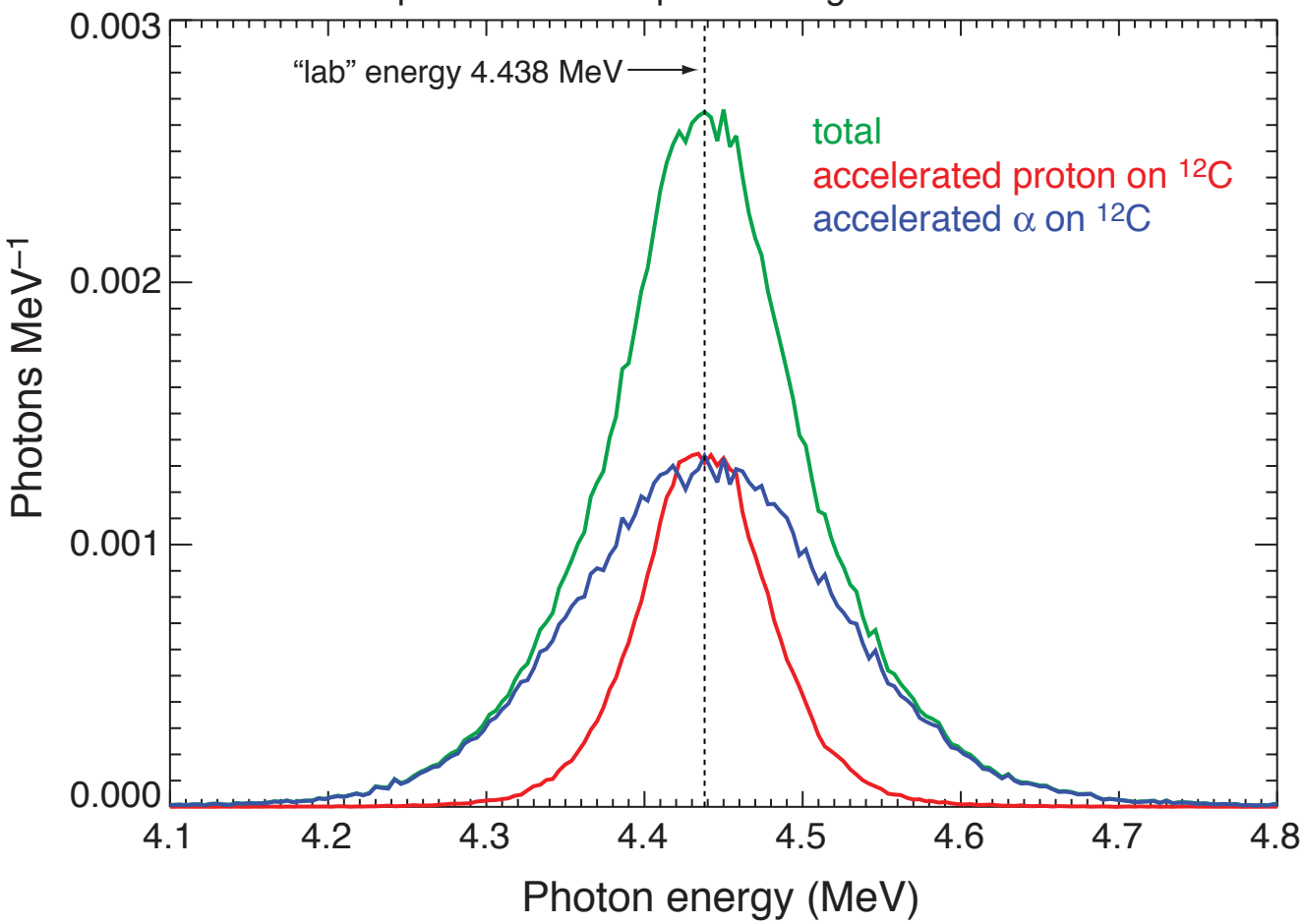

Nuclear Deexcitation Gamma-Ray Lines (cont.)
Line Shapes

Accelerated particle angular distribution and flare location affect observed Doppler shift

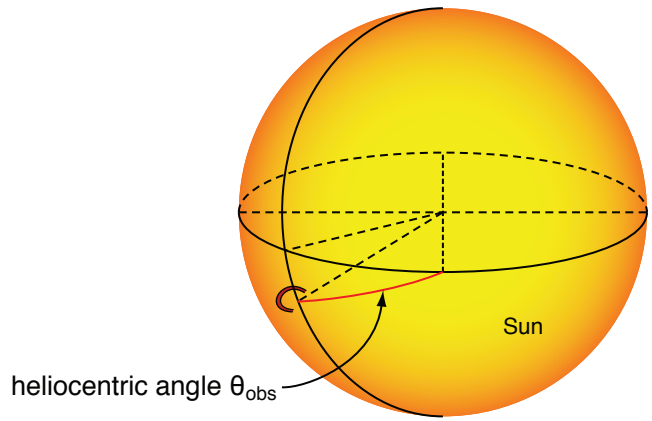

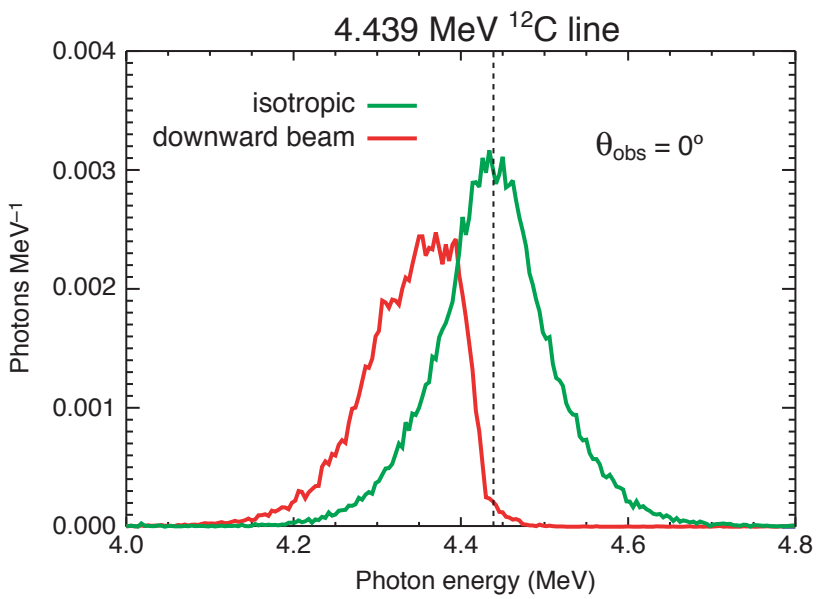

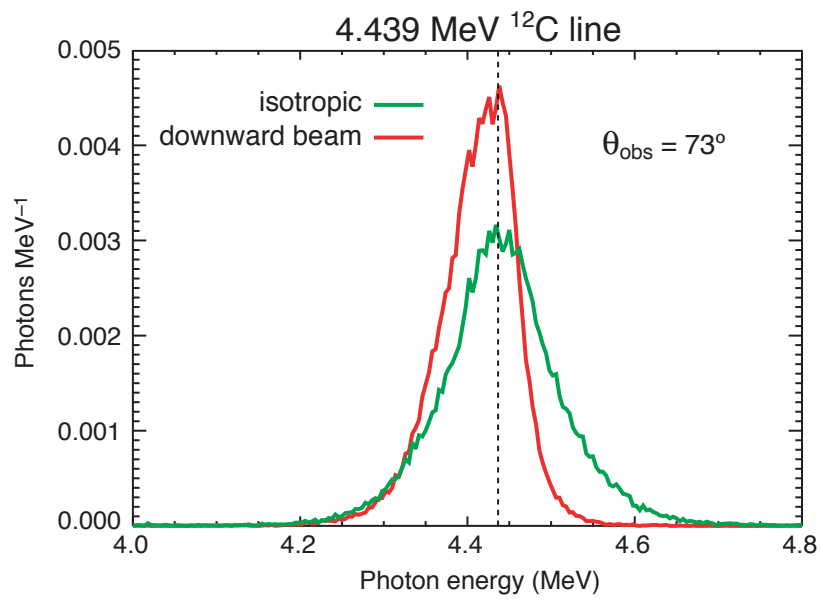

Nuclear Deexcitation Gamma-Ray Lines (cont.)
Total Spectrum

Narrow lines

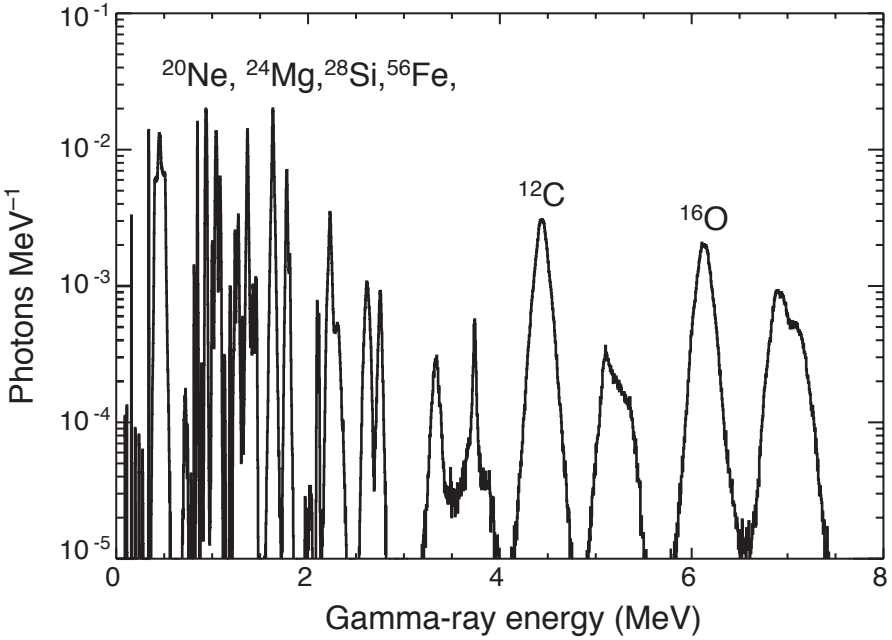

Broad lines

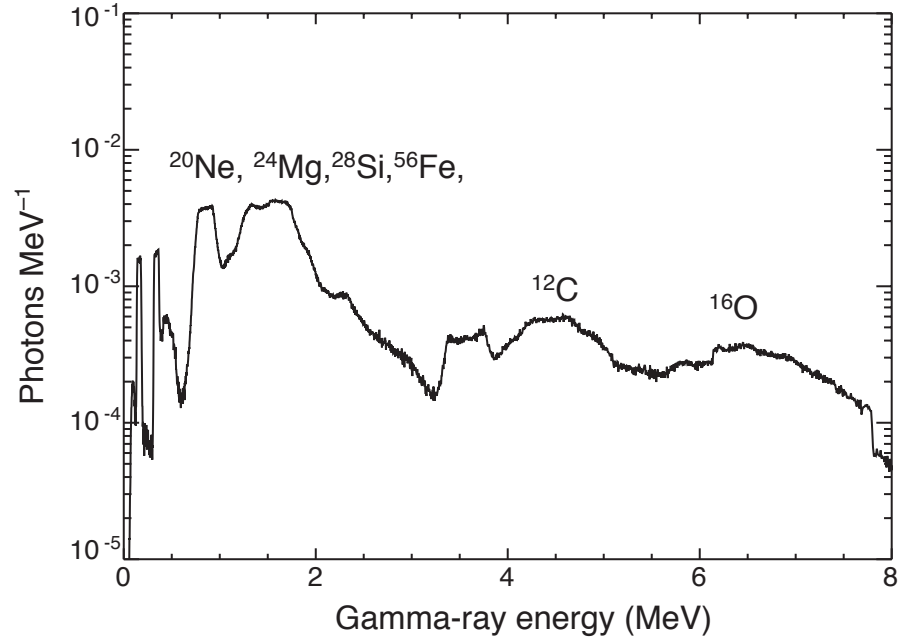

Nuclear continuum

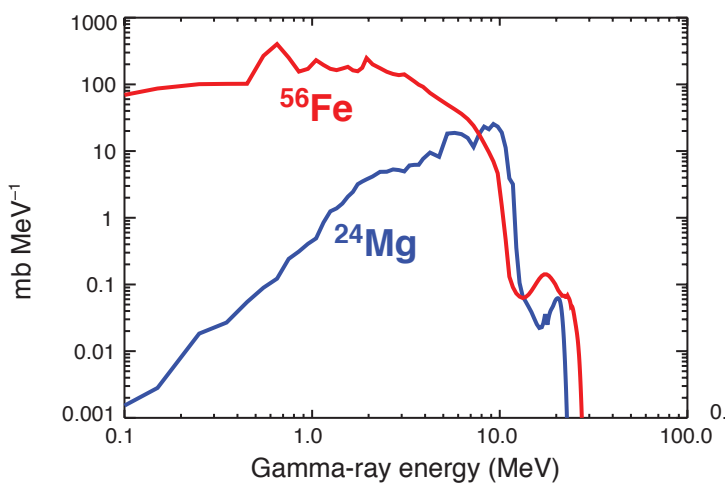

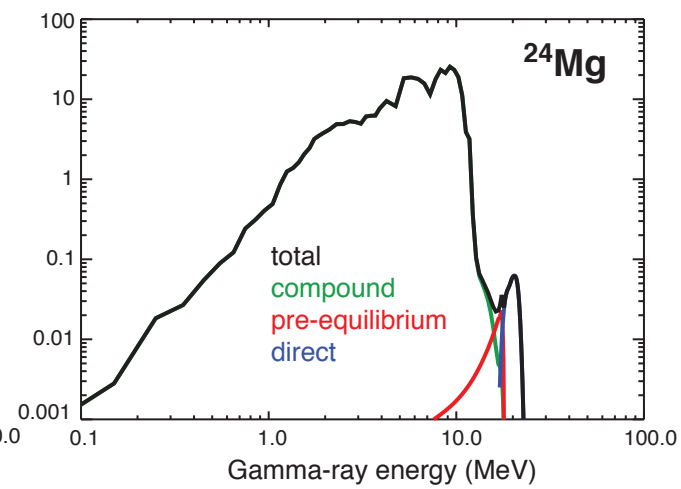

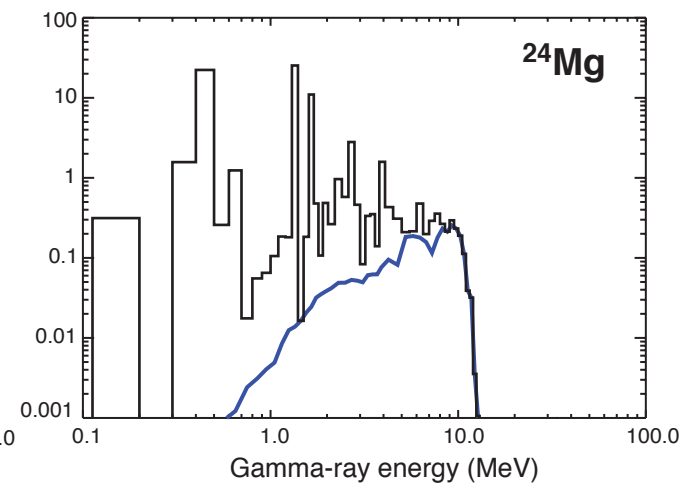

Nuclear Deexcitation Gamma-Ray Lines (cont.)
Energies of the Accelerated Ions

Line production cross sections

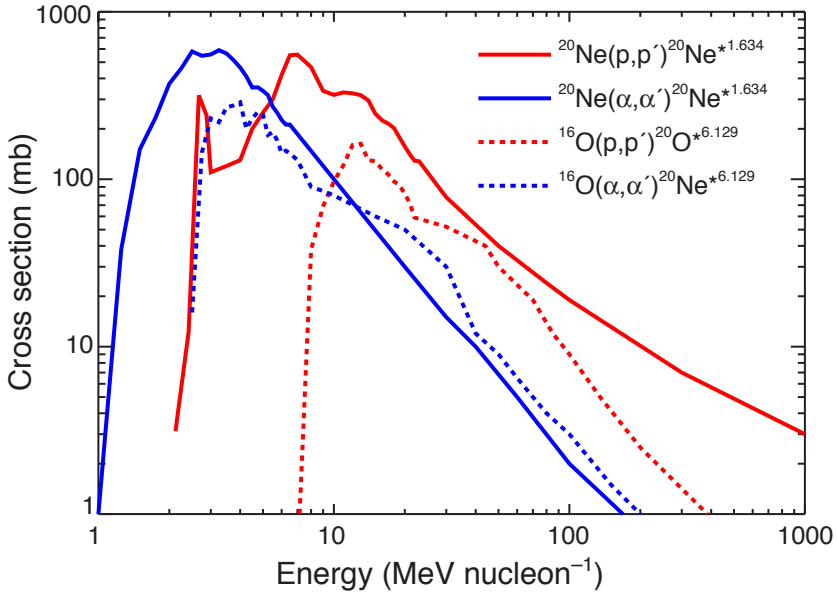

+

Accelerated ion initial kinetic energy distribution

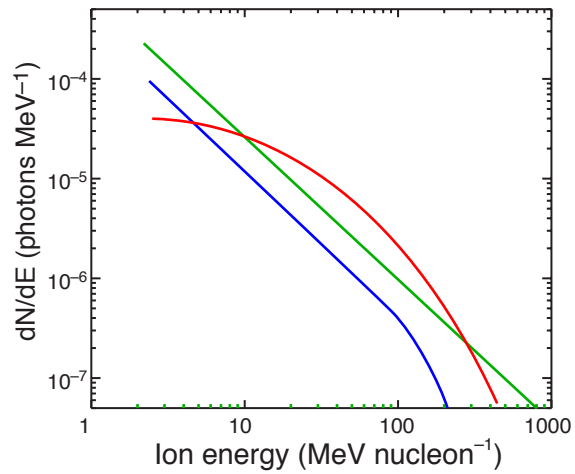

Power law
$dN/dE \propto E^{-s}$

PL with turnover
$dN/dE \propto E^{-s} \bullet \exp(-E/E_0)$

Bessel function
$dN/dE \propto K_2$

$$Q(E_0)\,\frac{dN}{dE} = n\,\frac{dN}{dE}(E_0)\int_0^{E_0} dE\,\frac{\sigma(E)}{dE/dl(E)}\,P(E_0,E)$$

Distribution of effective accelerated ion energies

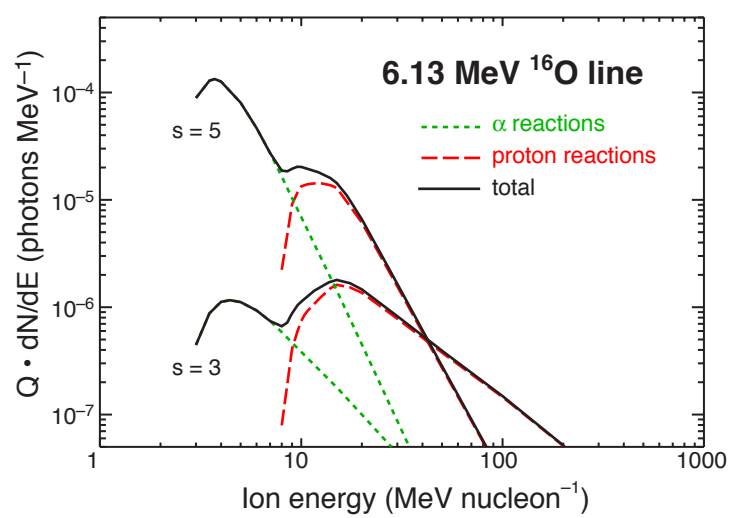

⇐

Effective accelerated ion energies

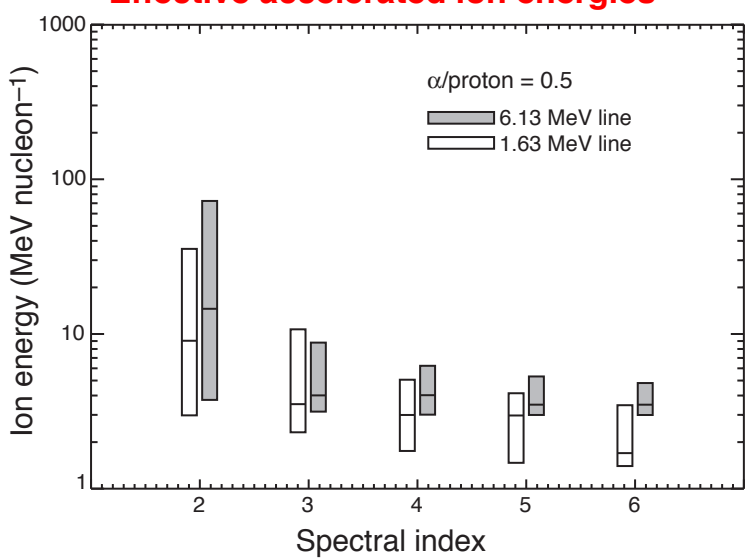

Nuclear Deexcitation Gamma-Ray Lines (cont.)
Yields

$$Q = n \int_0^{\infty} dE_0 \frac{dN}{dE}(E_0) \int_0^{E_0} dE \frac{\sigma(E)}{dE/dl(E)} P(E_0, E)$$

Yields and yield ratios

- sensitive measure of spectral steepness at ~2–10 MeV nucleon^{-1}
- ambient abundances

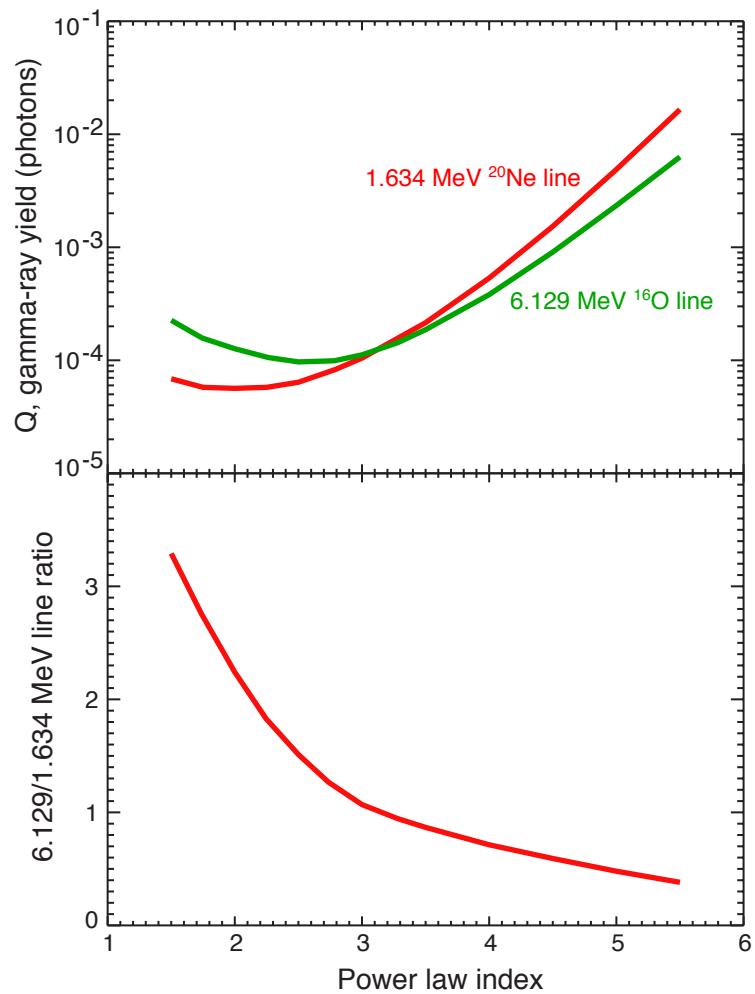

Nuclear Deexcitation Gamma-Ray Lines (cont.)
Production Depth

no significant attenuation due to Compton scattering

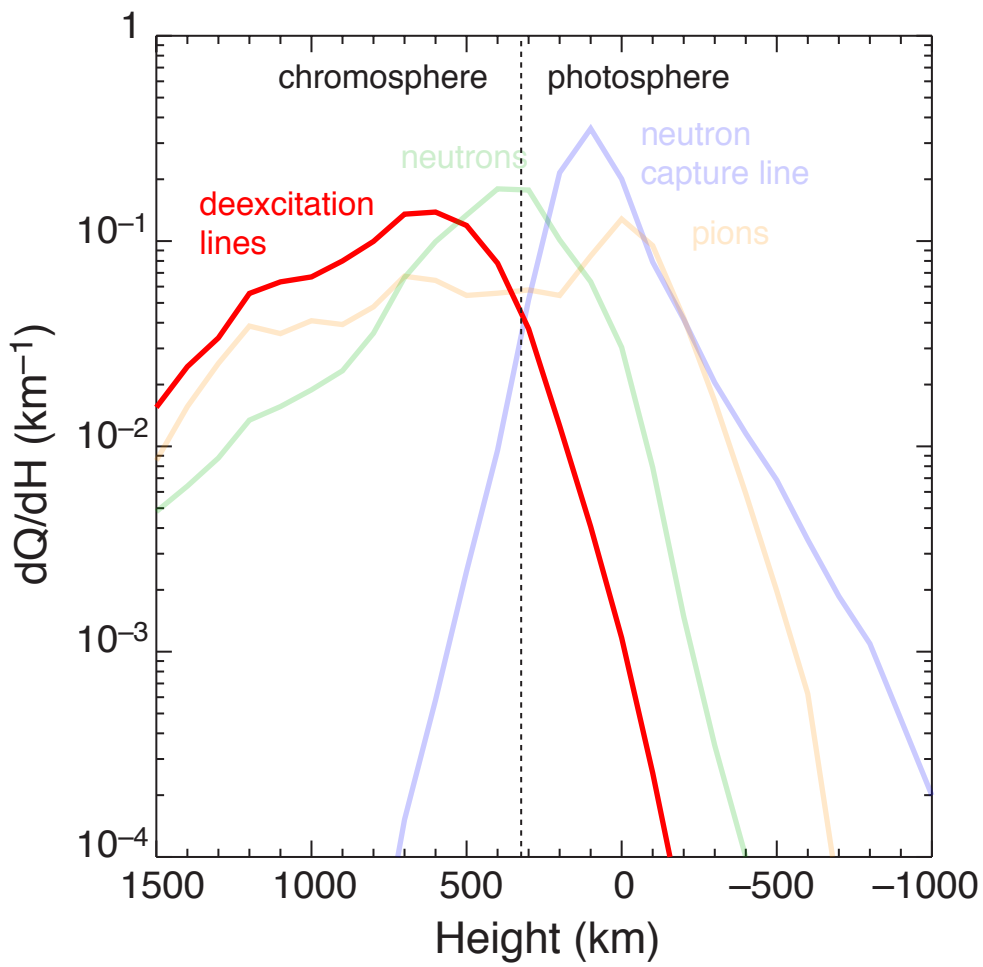

Positron Production and Annihilation

Radioactive positron emitters

$p \longrightarrow n + \nu + e^+$ (vs. e.c.: $p + e^- \longrightarrow n + \nu$)

$$\left.\begin{matrix} p \\ \alpha \end{matrix}\right\} + {}^{12}C \longrightarrow {}^{11}C + X$$

$$\xrightarrow[\tau]{} {}^{11}B + \nu + e^+$$

and the inverse reactions

	τ (sec)
^{16}O	9.6×10^{-11}
^{11}C	1800

Pions

$$\left.\begin{matrix} p + p \\ p + \alpha \end{matrix}\right\} \longrightarrow \pi^+ \xrightarrow[\tau_\pi]{} \mu^+ + \nu$$

$$\xrightarrow[\tau_\mu]{} e^+ + \nu + \bar{\nu}$$

	τ (sec)
π^+	3.8×10^{-8}
μ^+	2.1×10^{-6}

Other sources

$$\gamma + \gamma \longrightarrow e^+ + e^-$$

$$\gamma + B \longrightarrow e^+ + e^-$$

TABLE 3

POSITRON EMITTERS ORDERED BY LIFETIME

Positron Emitter	Positron Decay	Mean Life (sec)	Targets: Proton Reactions	Targets: Alpha Reactions
$^{16}O^*$	1	9.6×10^{-11}	^{16}O	^{16}O
$^{40}Ca^*$	1	3.1×10^{-9}	^{40}Ca	^{40}Ca
μ^+	1	2.2×10^{-6}	^{1}H, ^{4}He	^{1}H
^{12}N	1	0.016	^{12}C, ^{14}N, ^{16}O	
^{40}Sc	1	0.26	^{40}Ca	
^{54g}Co	1	0.28	^{54}Fe, ^{56}Fe	
^{28}P	1	0.39	^{28}Si	
^{50g}Mn	1	0.41	^{52}Cr	
^{32}Cl	1	0.43	^{32}S	
^{20}Na	1	0.65	^{20}Ne	
^{43}Ti	1	0.71		^{40}Ca
^{42g}Sc	1	0.98		^{40}Ca
^{39}Ca	1	1.24	^{40}Ca	^{36}Ar, ^{40}Ca
^{38m}K	1	1.34	^{40}Ca, ^{38}Ar	^{36}Ar, ^{40}Ca
^{30}S	1	1.73	^{32}S	
^{37}K	1	1.77	^{40}Ca	
^{34g}Cl	1	2.20	^{36}Ar, ^{40}Ca, ^{34}S	^{32}S, ^{36}Ar, ^{40}Ca
^{18}Ne	1	2.41	^{20}Ne	
^{35}Ar	1	2.54	^{36}Ar, ^{40}Ca	^{32}S, ^{36}Ar
^{24}Al	1	2.99	^{24}Mg	
^{26}Si	1	3.19	^{28}Si	
^{33}Cl	1	3.62	^{36}Ar, ^{40}Ca	
^{31}S	1	3.76	^{32}S, ^{36}Ar	^{28}Si, ^{32}S
^{58}Cu	0.98	4.62	^{58}Ni, ^{60}Ni	
^{22}Mg	1	5.57	^{24}Mg	
^{29}P	1	5.92	^{32}S, ^{36}Ar, ^{29}Si	
^{27}Si	1	5.96	^{28}Si, ^{27}Al, ^{32}S	^{24}Mg, ^{28}Si
^{26m}Al	1 1	9.16	^{26}Mg, ^{27}Al, ^{28}Si, ^{32}S, $^{26}Si(\beta^+)$	^{24}Mg, ^{28}Si, ^{32}S, ^{23}Na, ^{27}Al
^{25}Al	1	10.3	^{28}Si, ^{25}Mg, ^{32}S	
^{23}Mg	1	16.3	^{24}Mg, ^{28}Si, ^{23}Na	^{20}Ne, ^{24}Mg
^{19}Ne	1	24.9	^{20}Ne, ^{24}Mg	^{16}O, ^{20}Ne, ^{24}Mg
^{10}C	1	27.6	^{12}C, ^{14}N	
^{21}Na	1	32.4	^{24}Mg, ^{28}Si	
^{42m}Sc	1	89.4		^{40}Ca
^{17}F	1	93.1	^{20}Ne, ^{24}Mg	^{14}N, ^{20}Ne
^{14}O	1	102	^{14}N, ^{16}O	
^{59}Cu	1	118	^{60}Ni	^{58}Ni
^{54m}Co	1	126	^{54}Fe, ^{56}Fe	
^{61}Zn	0.99	129		^{58}Ni, ^{60}Ni
^{50m}Mn	1	151	^{52}Cr	
^{15}O	1	176	^{16}O, ^{20}Ne, ^{24}Mg, ^{15}N	^{12}C, ^{16}O, ^{20}Ne, ^{24}Mg
^{30}P	1	216	^{32}S, ^{36}Ar, ^{30}Si, $^{30}S(\beta^+)$	^{28}Si, ^{32}S, ^{36}Ar
^{38g}K	1	659	^{40}Ca, ^{38}Ar	^{36}Ar, ^{40}Ca
^{53}Fe	1	737	^{54}Fe, ^{56}Fe, ^{58}Ni, ^{60}Ni	^{54}Fe, ^{52}Cr
^{62}Cu	0.98	842		^{60}Ni
^{13}N	1	863	^{12}C, ^{14}N, ^{16}O, ^{20}Ne, ^{13}C	^{14}N, ^{16}O
^{11}C	1	$1.76\times10^{+3}$	^{11}C, ^{14}N, ^{16}O, ^{20}Ne	^{12}C, ^{14}N, ^{16}O, ^{20}Ne
^{52m}Mn	0.98	$1.83\times10^{+3}$	^{54}Fe, ^{56}Fe, ^{52}Cr, ^{58}Ni, ^{60}Ni	^{54}Fe
^{60}Cu	0.93	$2.03\times10^{+3}$	^{60}Ni	^{58}Ni, ^{60}Ni
^{34m}Cl	0.53	$2.77\times10^{+3}$	^{36}Ar, ^{40}Ca, ^{34}S	^{32}S, ^{36}Ar, ^{40}Ca
^{47}V	1	$2.82\times10^{+3}$		
^{63}Zn	0.93	$3.29\times10^{+3}$		^{60}Ni
^{49}Cr	1	$3.63\times10^{+3}$	^{52}Cr, ^{54}Fe, ^{56}Fe	
^{51}Mn	1	$4.00\times10^{+3}$	^{52}Cr, ^{54}Fe, ^{56}Fe, ^{60}Ni	
^{18}F	0.97	$9.50\times10^{+3}$	^{20}Ne, ^{24}Mg, ^{28}Si, ^{18}O, $^{18}Ne(\beta^+)$	^{16}O, ^{20}Ne, ^{24}Mg
^{45}Ti	0.86	$1.60\times10^{+4}$	^{52}Cr	
^{61}Cu	0.62	$1.77\times10^{+4}$		^{58}Ni, ^{60}Ni, $^{61}Zn(\beta^+)$
^{43}Sc	1	$2.02\times10^{+4}$	^{52}Cr, ^{43}Ti (β^+)	
^{52}Fe	1.55	$4.30\times10^{+4}$	^{54}Fe	
^{55}Co	0.77	$9.11\times10^{+4}$	^{56}Fe, ^{58}Ni, ^{60}Ni	^{54}Fe, ^{56}Fe
^{57}Ni	0.40	$1.87\times10^{+5}$	^{58}Ni, ^{60}Ni	^{54}Fe, ^{56}Fe, ^{58}Ni
^{52g}Mn	0.29	$6.97\times10^{+5}$	^{52}Cr, ^{54}Fe, ^{56}Fe, ^{58}Ni, ^{60}Ni	^{54}Fe
^{48}V	0.50	$1.99\times10^{+6}$	^{52}Cr, ^{54}Fe, ^{56}Fe, ^{58}Ni	
^{58}Co	0.15	$8.82\times10^{+6}$		^{56}Fe
^{56}Co	0.19	9.82×10^{6}	^{56}Fe, ^{58}Ni, ^{60}Ni	^{54}Fe, ^{56}Fe, ^{58}Ni
^{22}Na	0.91	$1.18\times10^{+8}$	^{24}Mg, ^{28}Si, ^{32}S, ^{23}Na, ^{22}Ne, ^{25}Mg, ^{27}Al	^{20}Ne, ^{24}Mg, ^{28}Si
^{26}Al	0.82	$3.26\times10^{+13}$	^{26}Mg, ^{27}Al, ^{28}Si, ^{32}S	^{24}Mg, ^{28}Si, ^{32}S

Kozlovsky, Lingenfelter & Ramaty 1987

Positron Production and Annihilation (cont.)

Production cross sections

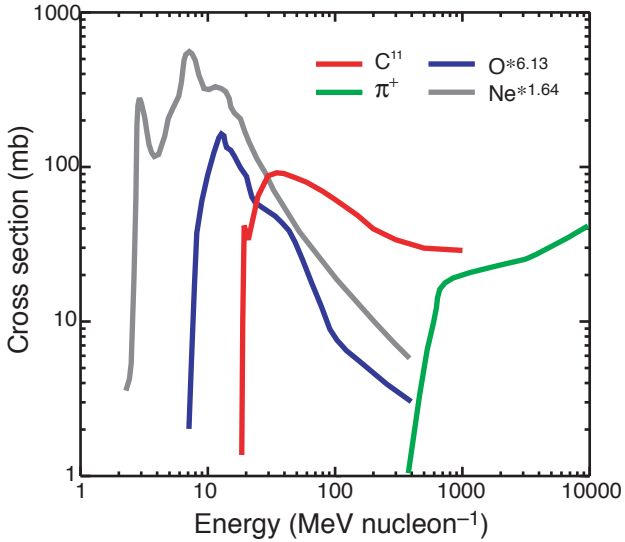

Effective accelerated ion energies

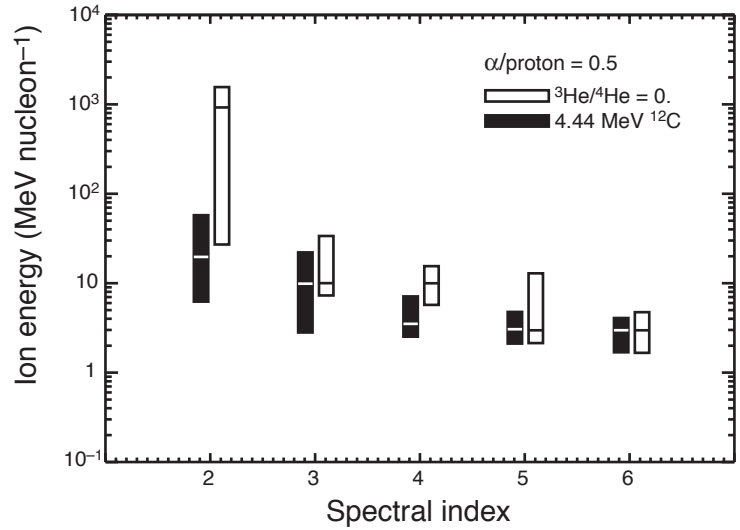

Positron yields

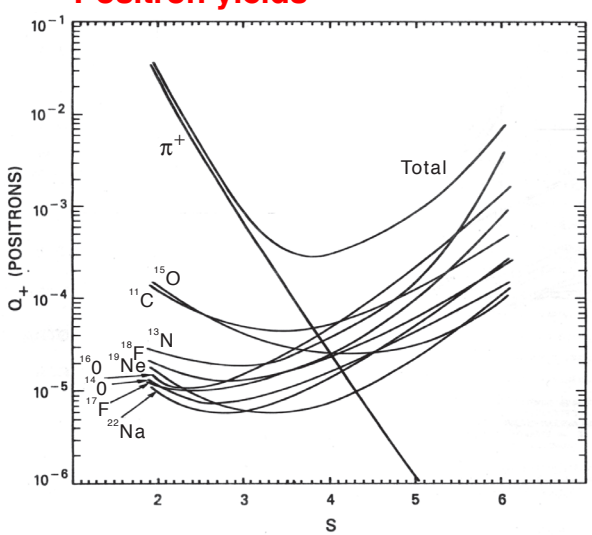

Yield ratios

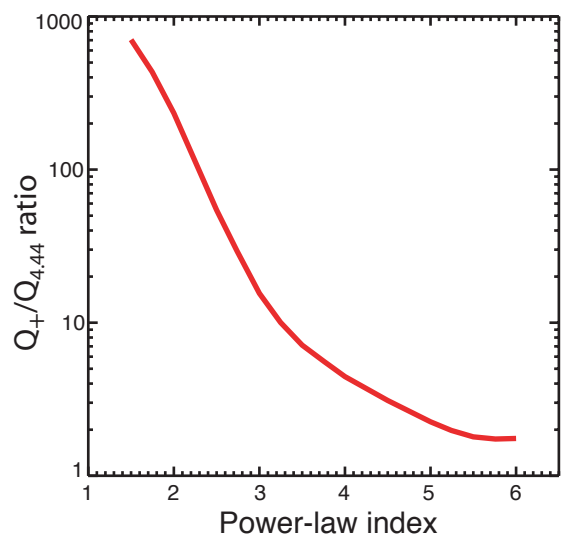

Positron Production and Annihilation (cont.)
Production Depth

attenuation due to Compton scattering depends on
accelerated-particle spectrum

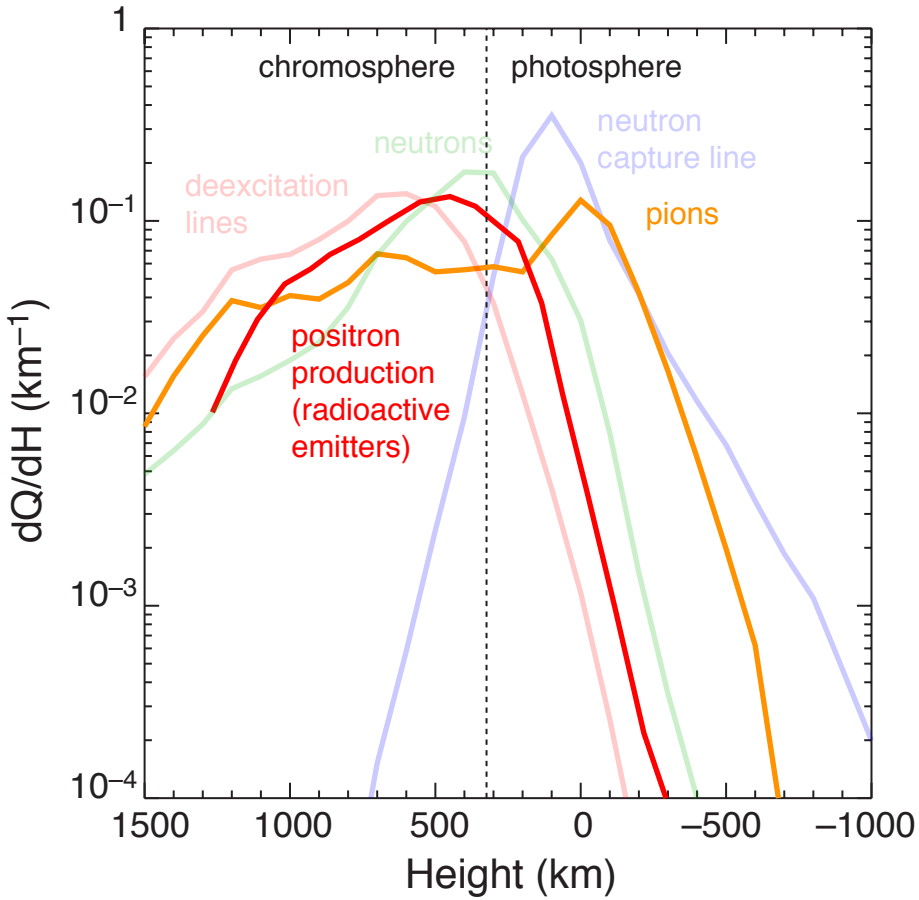

Positron Production and Annihilation (cont.)
Fate of Positrons

Direct annihilation with electrons ($e^+ + e^- \rightarrow 2\gamma_{511}$)

1. with free electrons (df)
2. with bound electrons of H and He (dab)

Positronium formation ($e^+ + e^- \rightarrow Ps$, $E_b = 6.8$ eV)

3. radiative combination with free electrons (rc)
4. charge exchange with H and He (ce)

$E_{th} = 13.6 - 6.8 = 6.8$ eV (H)
$24.6 - 6.8 = 17.8$ eV (He)

Two possible Ps spin configurations

$e^+\uparrow \; e^-\uparrow$ S = 1 "triplet" or "ortho" ^{3}Ps (3 states: $S_z = -1, 0, 1$)

$e^+\uparrow \; e^-\downarrow$ S = 0 "singlet" or "para" ^{1}Ps (1 state: $S_z = 0$)

⇒ always *formed* in 3:1 ratio

ground state, $n_{Ps} = 1$	$\tau_1 = 1.25 \times 10^{-10}$ s $\tau_3 = 1.4 \times 10^{-7}$ s
excited states, $n_{Ps} > 1$	$\tau_{ann} > \tau_{deexcite}$ $\Rightarrow$ always annihilates from ground state

Positron Production and Annihilation (cont.)

Positron Annihilation

Direct annihilation

$e^+ + e^- \rightarrow$

n_γ	
0	requires nucleus
1	
2	most probable $\rightarrow$ two 511 keV (= m_e) photons (a line)
3	suppressed by factors of α
4	
⋮	

Ps annihilation

CP invariance rule: for spin S and angular momentum L, the number of γ rays n_γ is given by

$$(-1)^{n_\gamma} = (-1)^{L+S}$$

for ground state $n_{Ps} = 1$, $L = 0$, so

$S = 0 \Longrightarrow n_\gamma = 2, 4, 6, \ldots$

$S = 1 \Longrightarrow n_\gamma = 3, 5, 7, \ldots$

lowest orders dominate

$S = 0 \longrightarrow$ two 511 kev photons (a line)

$S = 1 \longrightarrow$ three <511 kev γ rays (a continuum)

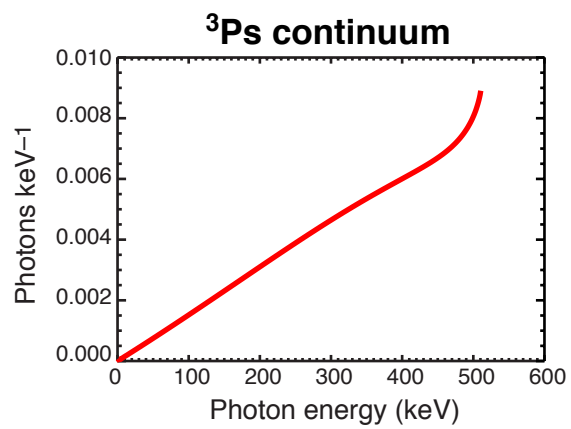

Positron Production and Annihilation (cont.)
Positronium Quenching

At sufficiently-high density, collisions with ambient particles (H, He & e^-) may disturb Ps before annihilation

Because of its longer lifetime, this is relevant only for ^{3}Ps

There are 2 types of quenching:

1. ^{3}Ps ionization reducing 3γ and increasing 2γ
2. conversion of ^{3}Ps to ^{1}Ps (spin flip) reducing 3γ and increasing 2γ

Density estimate:

quenching rate ($n_H \sigma v$) must be greater than annihilation rate ($1/\tau_3$), so, with $v = \sqrt{kT/m_e}$,

$$n_H > (\sigma\, \tau_3 \sqrt{kT/m_e})^{-1}$$

for $T = 10^4$ K and $\sigma = 5 \times 10^{-16}$ cm^2, $n_H \gtrsim 10^{14}$ cm^{-3}

Positron Production and Annihilation (cont.)
Slowing-Down of Positrons

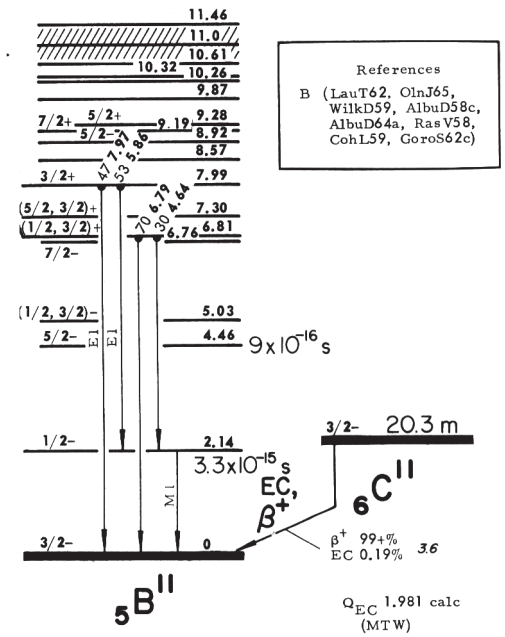

positron $KE_{max} = \Delta M - m_{e^+}$

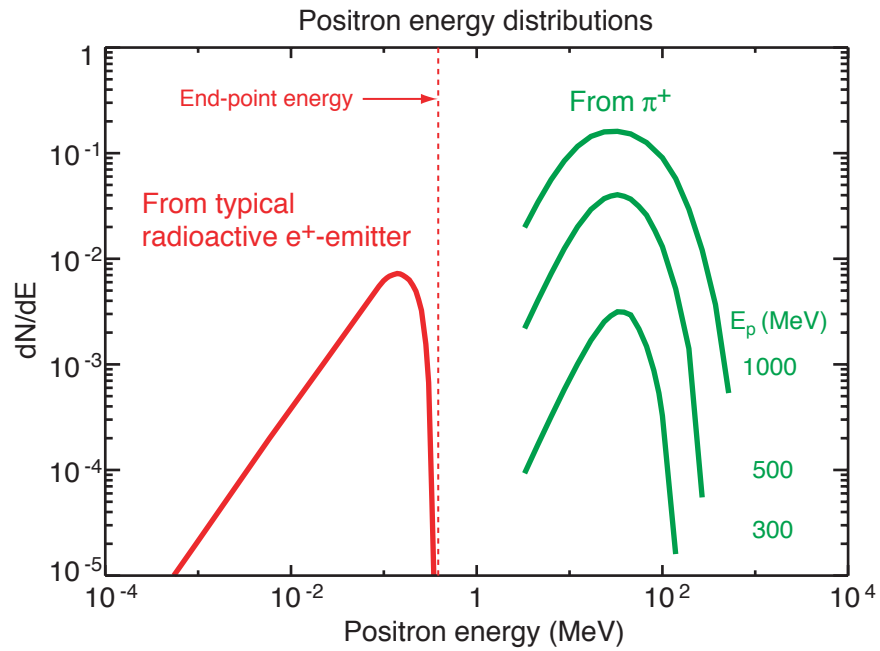

Initial e^+ energies are 100 keV – 100 MeV

The dominant e^+ interactions above a few hundred eV involve energy loss:

1. Continuous with free electrons
2. Discrete via excitation and ionization of H and He

Below ~100 eV, Ps formation via charge exchange in-flight (ifce) becomes significant

Thermalized e^+ can annihilate via all four processes: daf, dab, rc, ce

Quenching can reduce the ^{3}Ps continuum and increase the line yield

Positron Production and Annihilation (cont.)

Positron Fate

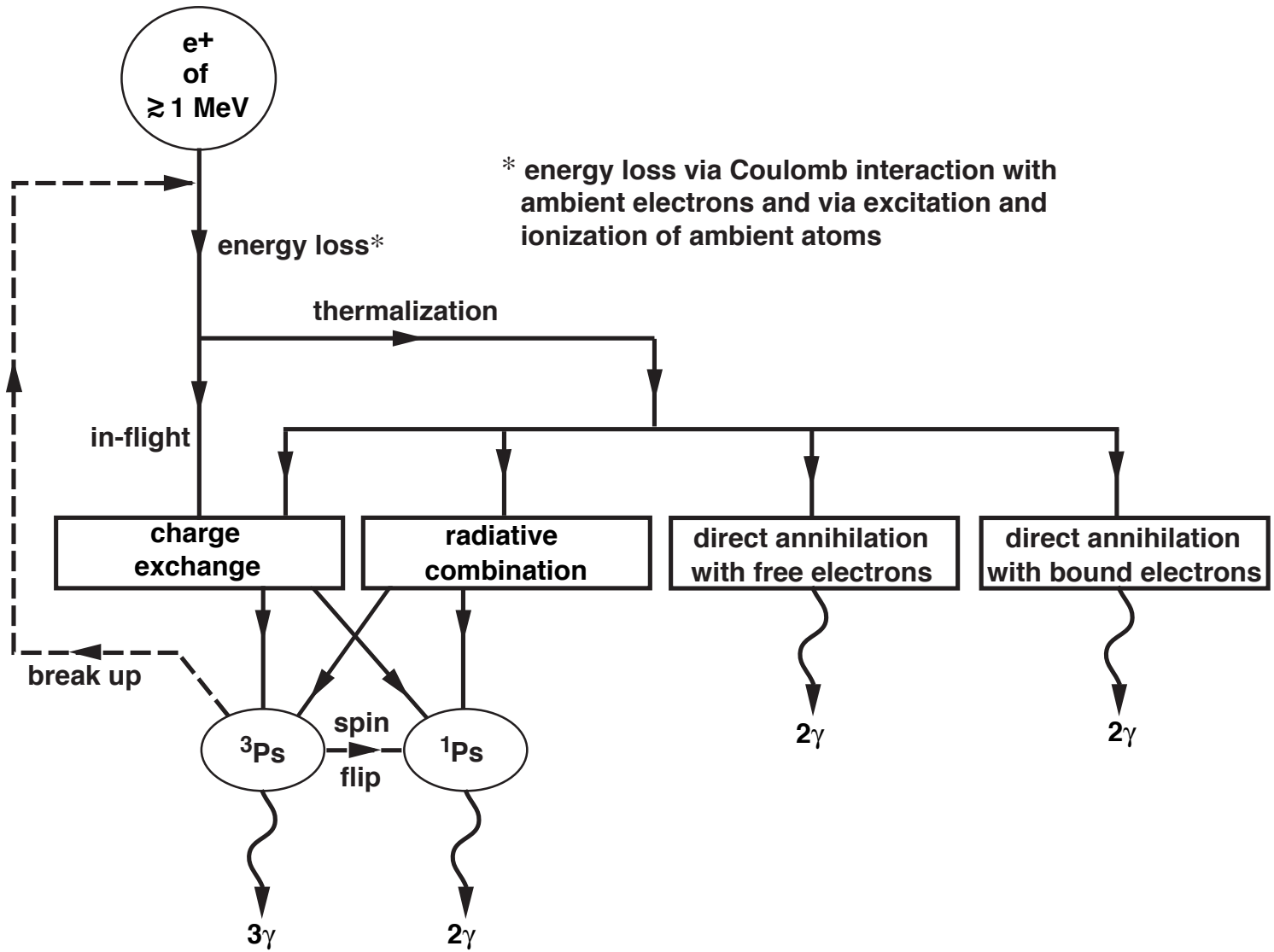

Positron Production and Annihilation (cont.)
Interaction Cross Sections

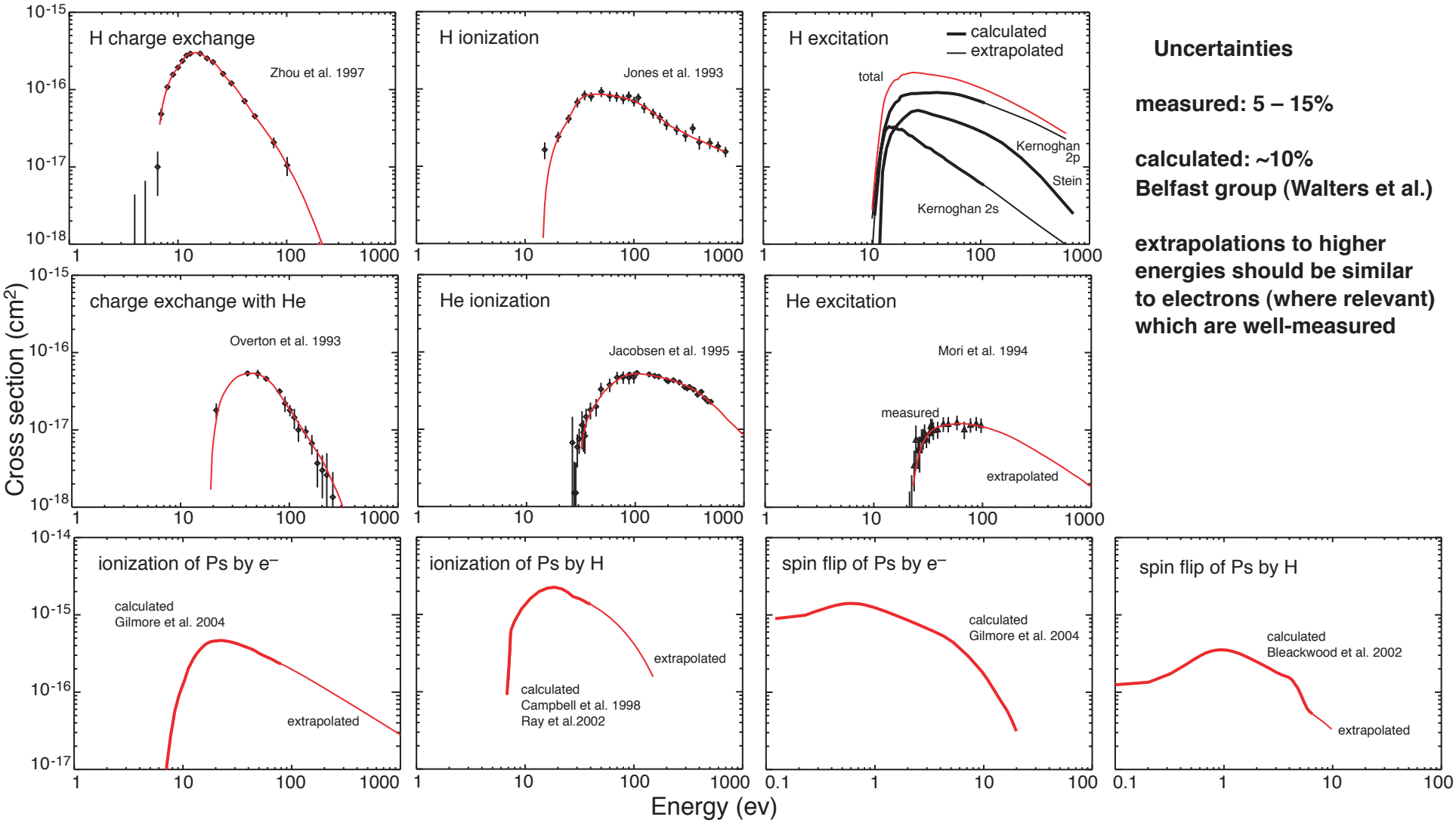

Uncertainties

measured: 5 – 15%

calculated: ~10%
Belfast group (Walters et al.)

extrapolations to higher energies should be similar to electrons (where relevant) which are well-measured

Positron Production and Annihilation (cont.)

Monte Carlo Simulation of Ps Formation In-Flight

Monte Carlo simulation includes:

- continuous energy loss to electrons
- discrete losses via ionization and excitation
- 2nd generation e^+ from ionization quenching of Ps

Provides:

1. fraction forming Ps in flight, f_1 & f_2
2. energy distribution of 1st and 2nd generation Ps
3. resulting ^{1}Ps annihilation line profiles

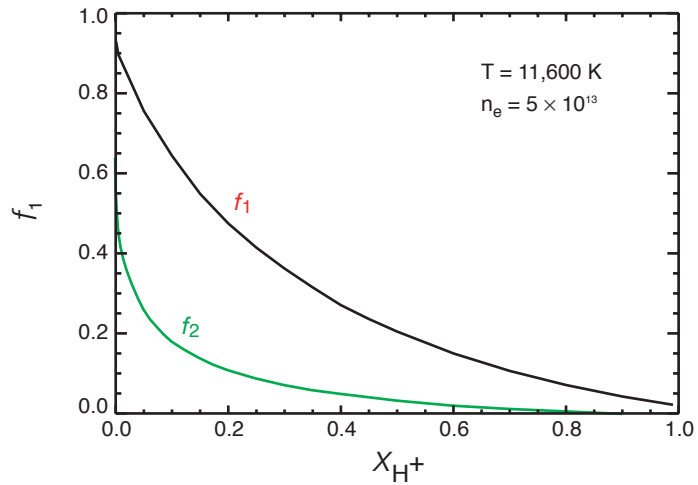

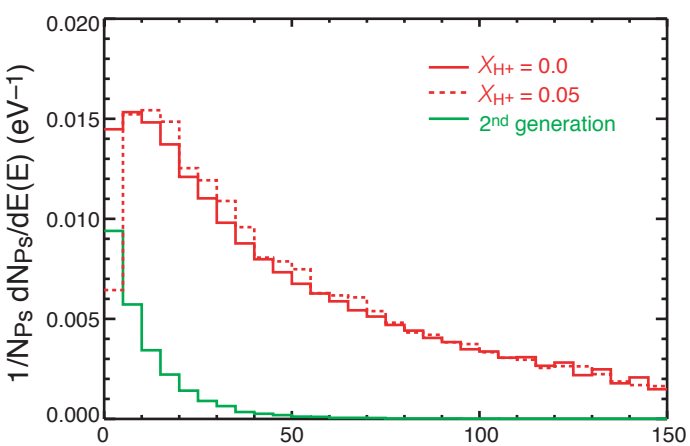

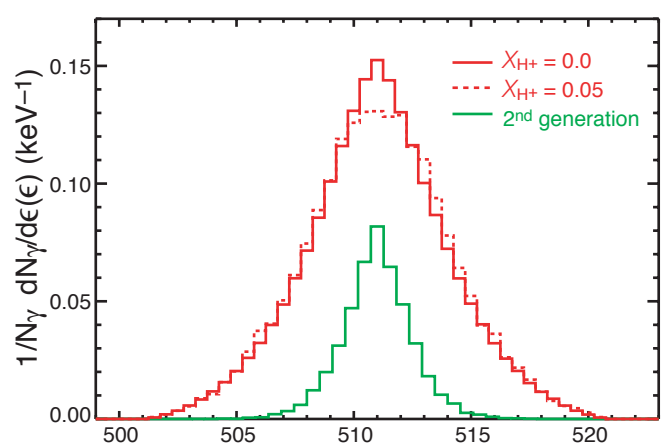

Line shapes are NOT Gaussian

1st gen. FWHM ≈ 6.1 keV

2nd gen. FWHM ≈ 2.6 keV

Positron Production and Annihilation (cont.)
Line Shapes from Annihilation

direct

daf → (both particles are Maxwellian) → (line shape is Gaussian) → FWHM ≈ $1.1\sqrt{T_4}$ keV

dab → (depends on momentum of atomic e^-)

low temp → (depends only atomic e^-) → (line shape is ~ Gaussian) → FWHM ≈ 1.4 keV (H)
FWHM ≈ 2.5 keV (He)

high temp → (depends only e^+ distribution) → (line shape is Gaussian) → FWHM ∝ $\sqrt{T}$

→ (line shape is ~ Gaussian) → $\Gamma_{tot}^2 = \Gamma_{lo}^2 + \Gamma_{hi}^2$

Ps formation

ce → (Ps distribution is NOT Maxwellian) → (line shape is NOT Gaussian) →

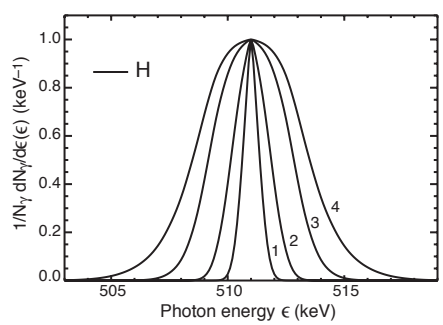

T (K)	FWHM (keV)
1) 6×10^3	0.8
2) 2×10^4	1.7
3) 1×10^5	3.5
4) 4×10^5	5.0

rc → (Ps remains Maxwellian) → (line shape is Gaussian) → FWHM ≈ $1.1\sqrt{T_4}$ keV

---

in-flight ce → (Ps distribution is NOT Maxwellian) → (line shape is NOT Gaussian) → FWHM ≈ 6.1 keV (1st generation)
FWHM ≈ 2.6 keV (2nd generation)

Positron Production and Annihilation (cont.)

Thermal Interaction Rates

$$\lambda = \left(\frac{\sqrt{m_1 m_2}}{2\pi kT} \right)^3 \int d^3\mathbf{v_1}\, d^3\mathbf{v_2}\ \exp\left(-\frac{m_1 v_1^2}{2kT}\right) \exp\left(-\frac{m_2 v_2^2}{2kT}\right) v\, \sigma(\mathbf{v_1}, \mathbf{v_2})$$

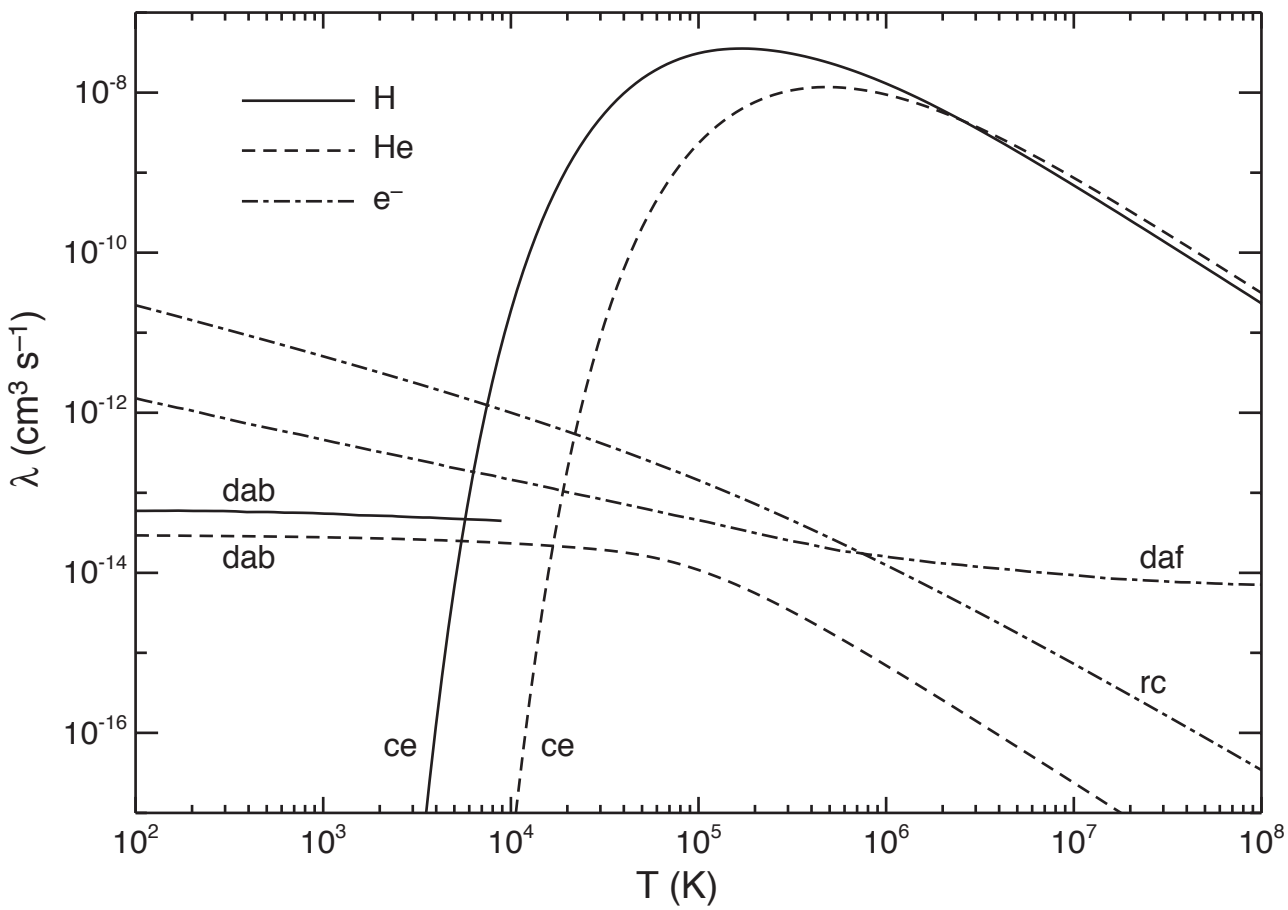

Positron Production and Annihilation (cont.)

^{3}Ps Quenching Rates

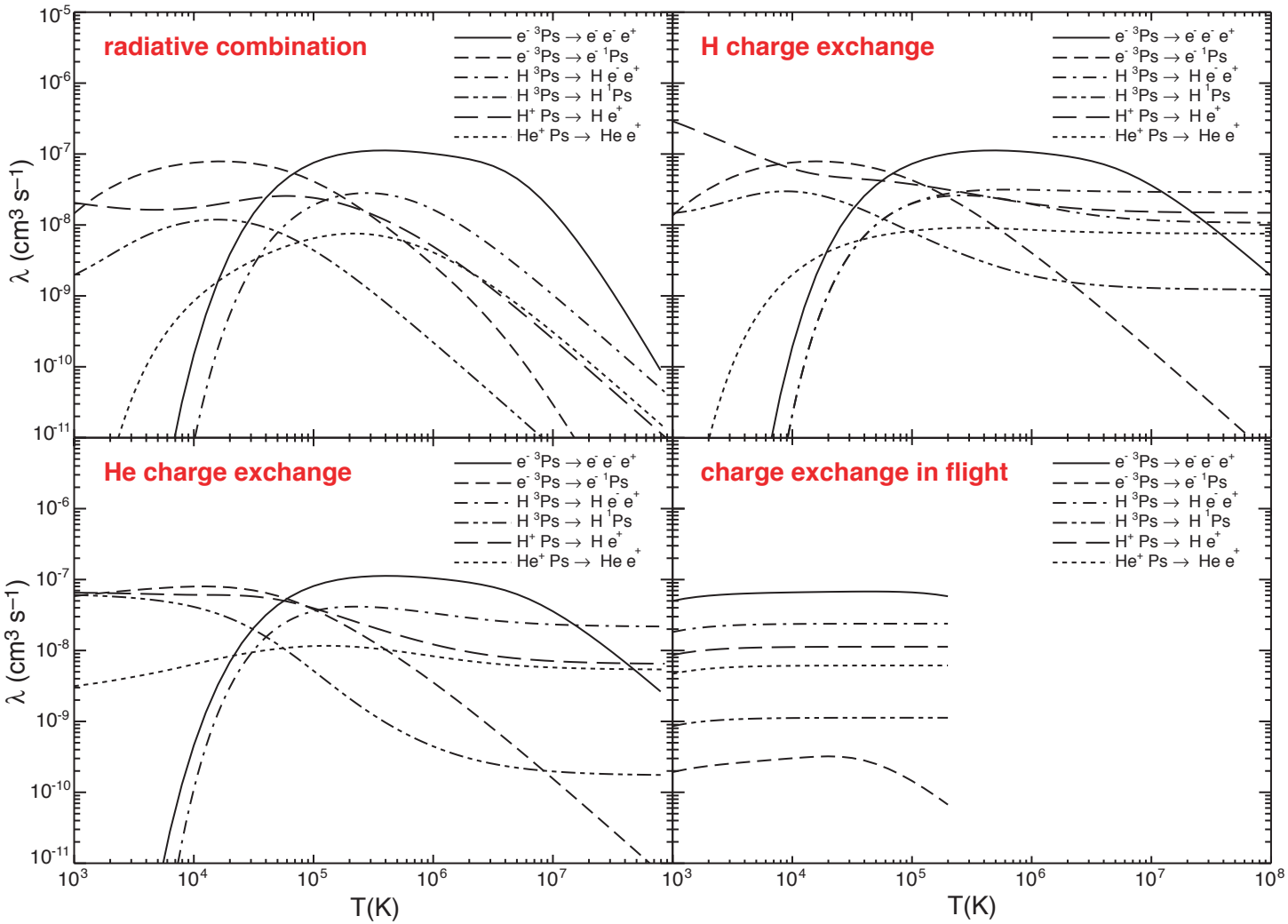

Positron Production and Annihilation (cont.)

Continuity Equations

rate of change of ^{3}Ps from ifce

^{3}Ps formation rate

^{3}Ps quenching rate

^{3}Ps annihilation rate

$$
\begin{aligned}
\frac{\partial N_3^{ifce}}{\partial t} &= \frac{3}{4} f_1 Q_+ - N_3^{ifce} R_{3\to x}^{ifce} - \frac{N_3^{ifce}}{\tau_3} = 0 \\
\frac{\partial N_3^{2g}}{\partial t} &= \frac{3}{4} f_2 N_3^{ifce} R_{3\to 0}^{ifce} - N_3^{2g} R_{3\to x}^{2g} - \frac{N_3^{2g}}{\tau_3} = 0 \\
\frac{\partial N_3^{Hce}}{\partial t} &= \frac{3}{4} N_+ R^{Hce} - N_3^{Hce} R_{3\to x}^{Hce} - \frac{N_3^{Hce}}{\tau_3} = 0 \\
\frac{\partial N_3^{Hece}}{\partial t} &= \frac{3}{4} N_+ R^{Hece} - N_3^{Hece} R_{3\to x}^{Hece} - \frac{N_3^{Hece}}{\tau_3} = 0 \\
\frac{\partial N_3^{rc}}{\partial t} &= \frac{3}{4} N_+ R^{rc} - N_3^{rc} R_{3\to x}^{rc} - \frac{N_3^{rc}}{\tau_3} = 0 \\
\frac{\partial N_1^{ifce}}{\partial t} &= \frac{1}{4} f_1 Q_+ + N_3^{ifce} R_{3\to 1}^{ifce} - \frac{N_1^{ifce}}{\tau_1} = 0 \\
\frac{\partial N_1^{2g}}{\partial t} &= \frac{1}{4} f_2 N_3^{ifce} R_{3\to 0}^{ifce} + N_3^{2g} R_{3\to 1}^{2g} - \frac{N_1^{2g}}{\tau_1} = 0 \\
\frac{\partial N_1^{Hce}}{\partial t} &= \frac{1}{4} N_+ R^{Hce} + N_3^{Hce} R_{3\to 1}^{Hce} - \frac{N_1^{Hce}}{\tau_1} = 0 \\
\frac{\partial N_1^{Hece}}{\partial t} &= \frac{1}{4} N_+ R^{Hece} + N_3^{Hece} R_{3\to 1}^{Hece} - \frac{N_1^{Hece}}{\tau_1} = 0 \\
\frac{\partial N_1^{rc}}{\partial t} &= \frac{1}{4} N_+ R^{rc} + N_3^{rc} R_{3\to 1}^{rc} - \frac{N_1^{rc}}{\tau_1} = 0 \\
\frac{\partial N_+}{\partial t} &= (1-f_1) Q_+ + (1-f_2) N_3^{ifce} R_{3\to 0}^{ifce} + N_3^{2g} R_{3\to 0}^{2g} \\
&\quad + N_3^{Hce} R_{3\to 0}^{Hce} + N_3^{Hece} R_{3\to 0}^{Hece} + N_3^{rc} R_{3\to 0}^{rc} \\
&\quad - N_+ (R^{Hce} + R^{Hece} + R^{rc} + R^{Hdab} + R^{Hedab} + R^{daf}) = 0.
\end{aligned}
$$

$$
\begin{aligned}
Q_{2\gamma} &= 2N_+ \left(R^{Hdab} + R^{Hedab} + R^{daf} \right) + \\
&\quad + \frac{2}{\tau_1} \left(N_1^{ifce} + N_1^{Hce} + N_1^{Hece} + N_1^{rc} + N_1^{2g} \right)
\end{aligned}
$$

$$
Q_{3\gamma} = \frac{3}{\tau_3} \left(N_3^{ifce} + N_3^{Hce} + N_3^{Hece} + N_3^{rc} + N_3^{2g} \right)
$$

Positron Production and Annihilation (cont.)

f_{511}

the number of 511 keV photons per positron

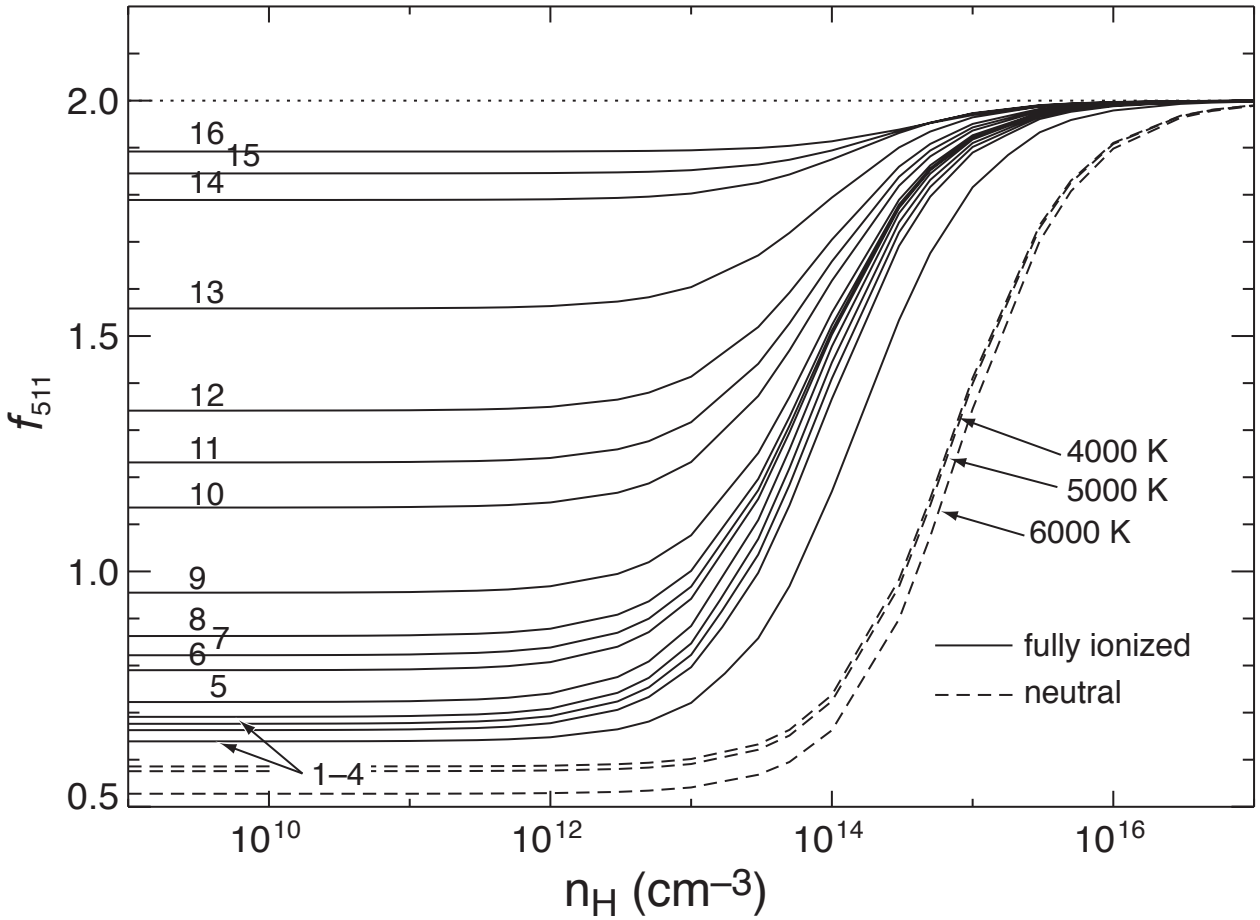

	T (K)		
1.	2×10^3	9.	2×10^5
2.	5×10^3	10.	5×10^5
3.	7×10^3	11.	7×10^5
4.	1×10^4	12.	1×10^6
5.	2×10^4	13.	2×10^6
6.	5×10^4	14.	5×10^6
7.	7×10^4	15.	7×10^6
8.	1×10^5	16.	1×10^7

Positron Production and Annihilation (cont.)
Combined Line Shapes

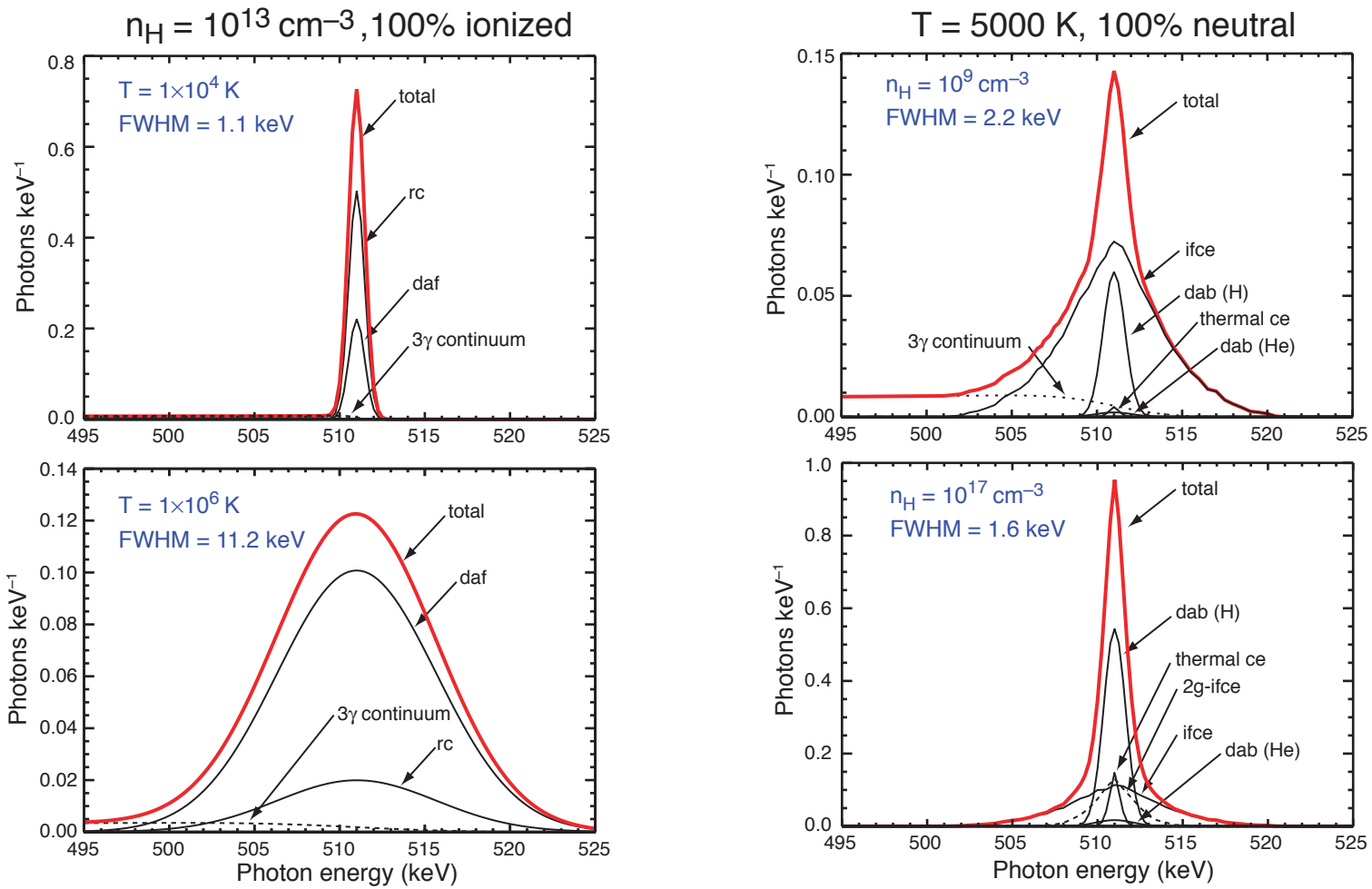

The line shape is NOT Gaussian!

Positron Production and Annihilation (cont.)

Vernazza Line Shapes and $Q_{3\gamma}/Q_{2\gamma}$ Ratio

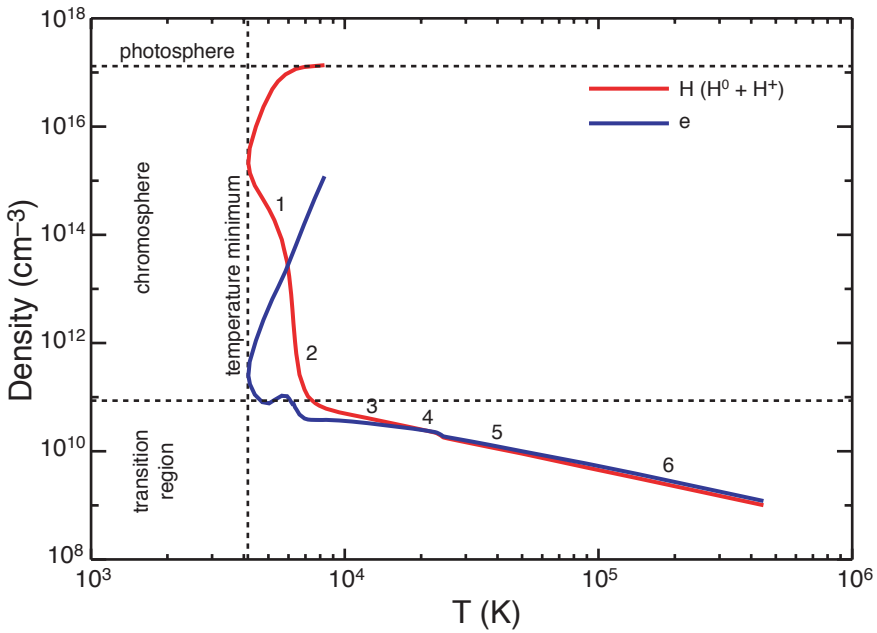

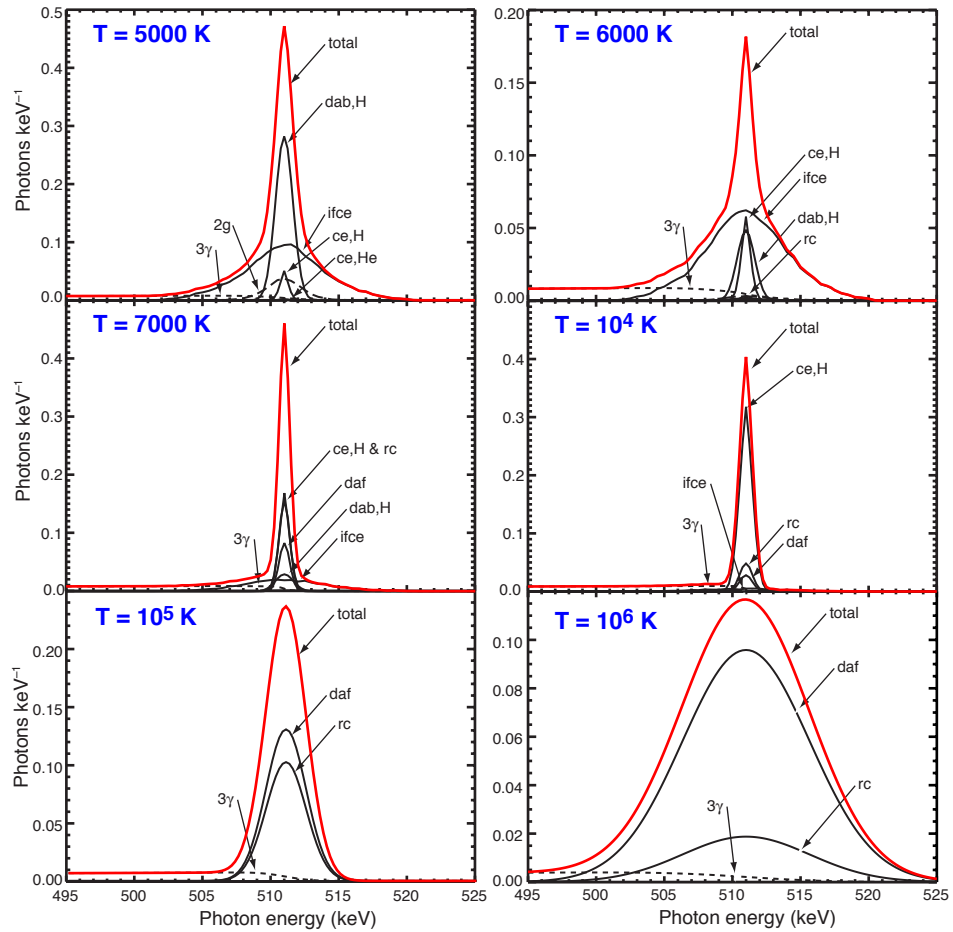

NEUTRONS

Neutron production

$p + p \longrightarrow n + \ldots$

$p + {}^4He \longrightarrow n + \ldots$

$\alpha + \alpha \longrightarrow n + \ldots$

$\left.\begin{matrix} p \\ \alpha \end{matrix}\right\} + {}^{12}C \longrightarrow n + \ldots$

and inverse reactions

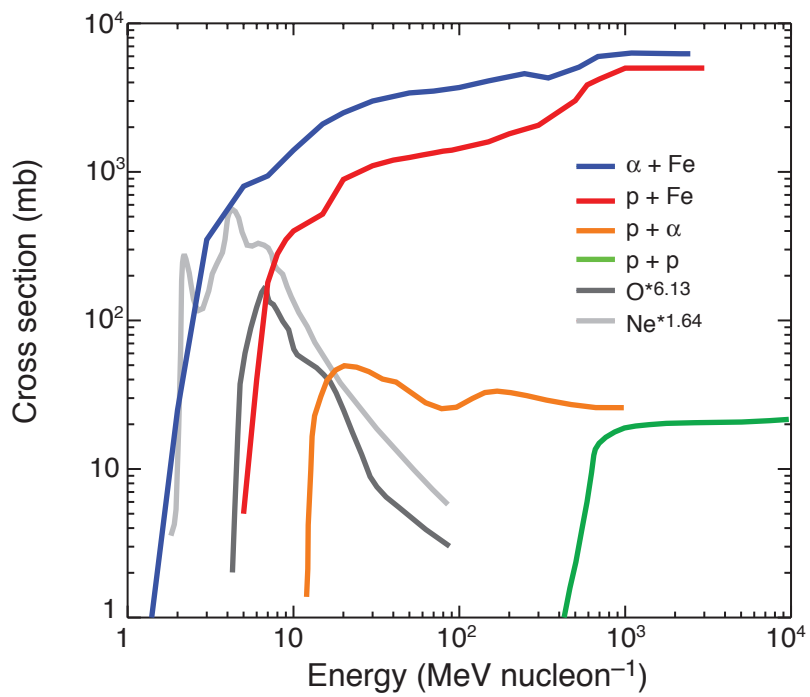

Neutrons are "detectable" either directly or indirectly

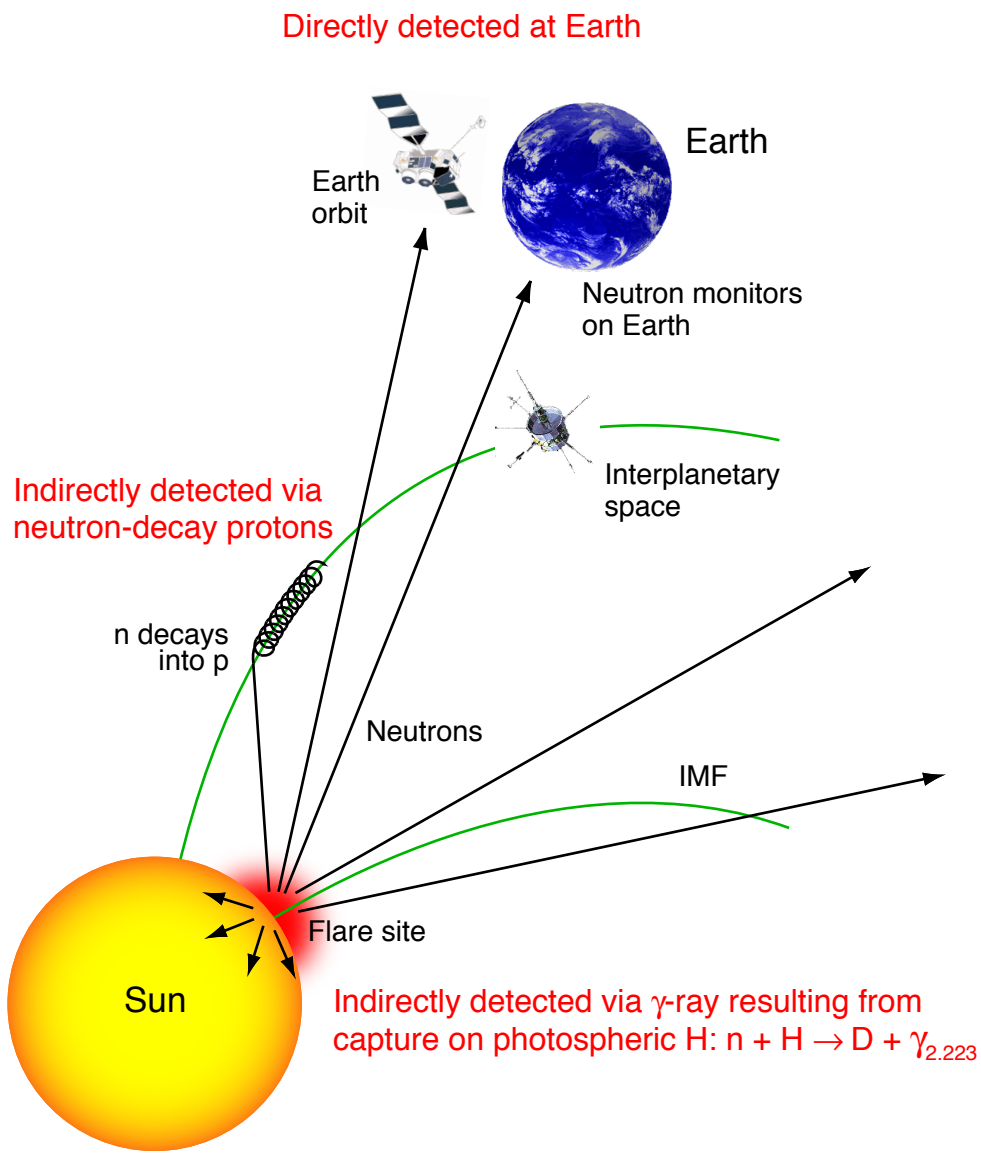

NEUTRON PRODUCTION (cont.)

Energy Spectra

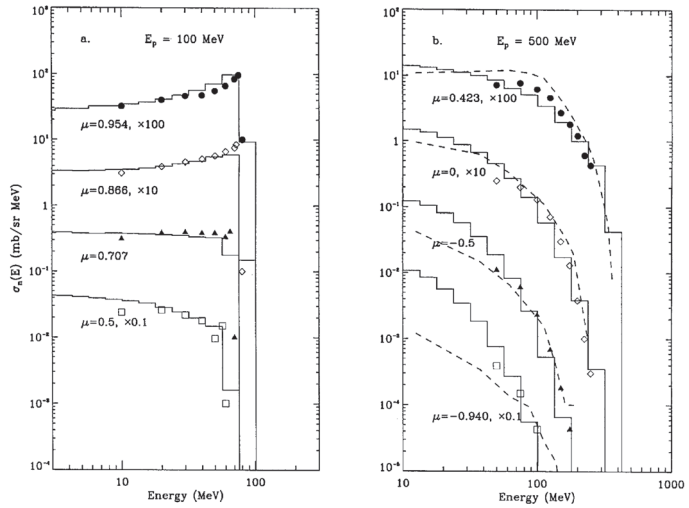

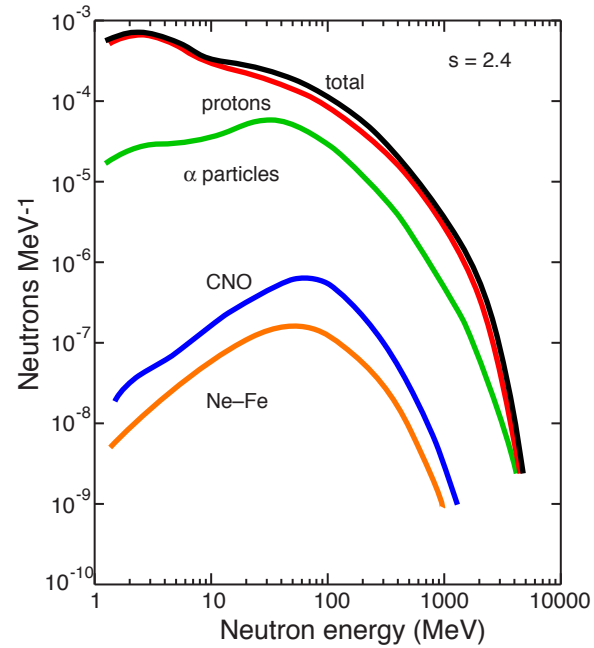

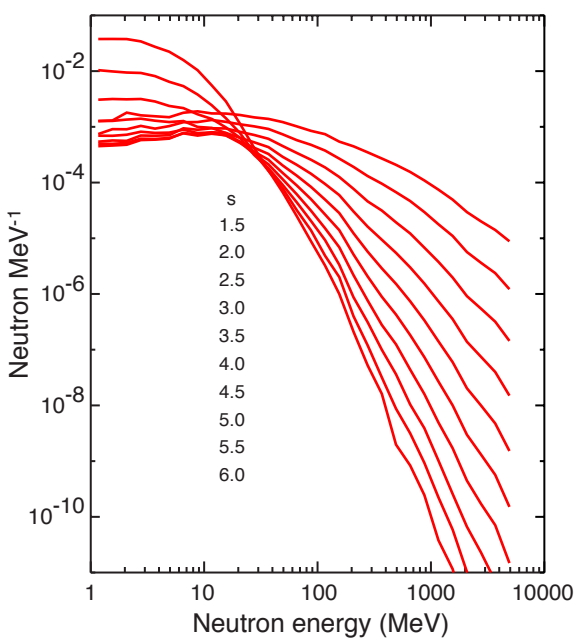

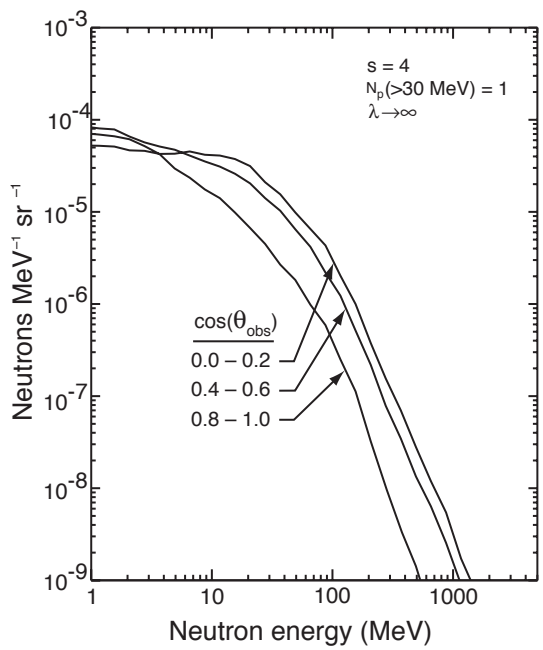

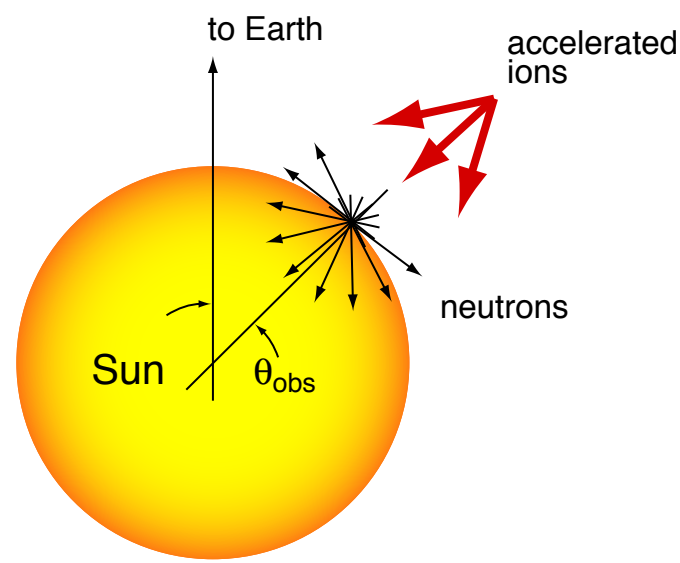

NEUTRON PRODUCTION (cont.)

Energy Spectra

Neutron lifetime (τ_{mean} = 886 s) alters kinetic energy spectrum with distance from Sun

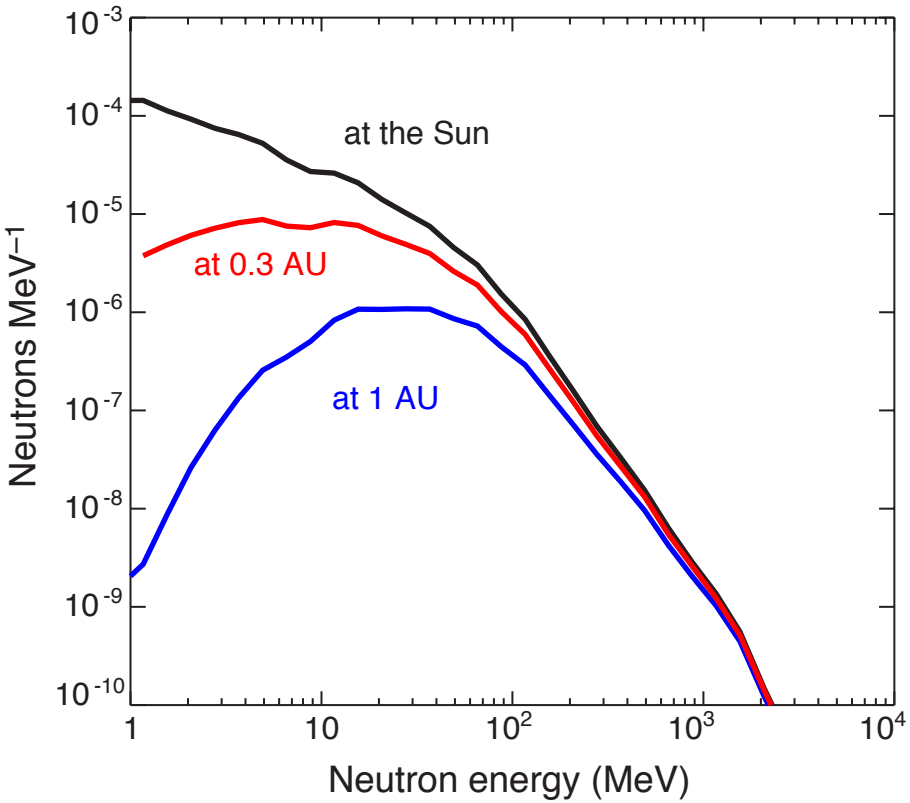

Differing neutron velocities result in time-dependent arriving kinetic spectra due to velocity dispersion

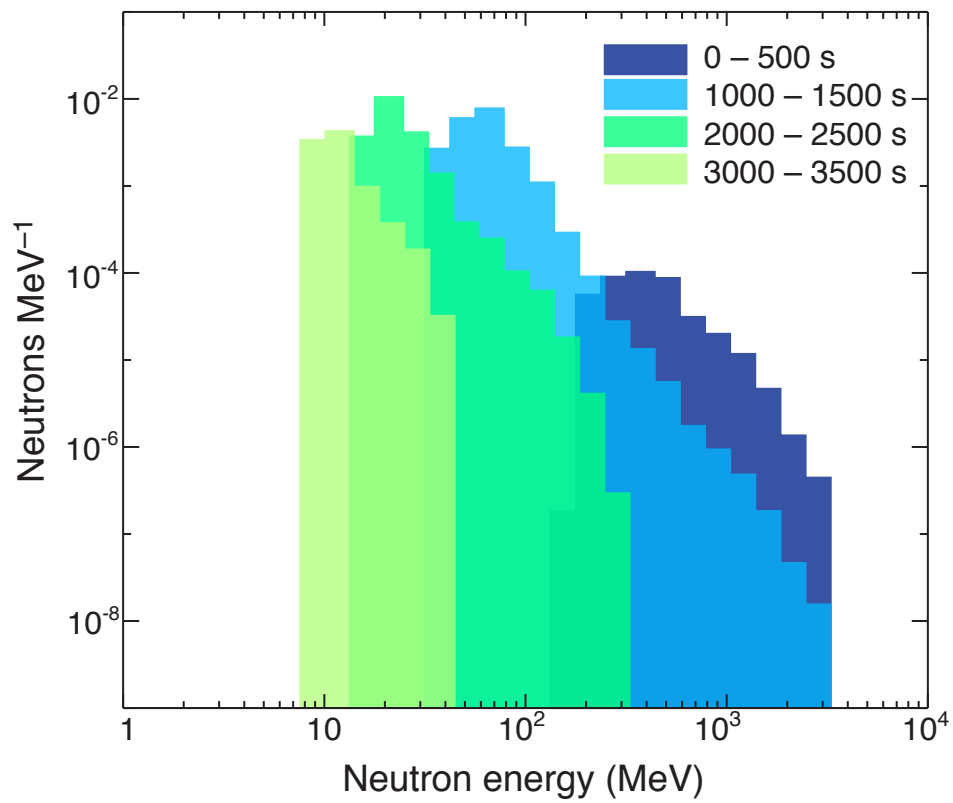

2.223 MeV NEUTRON-CAPTURE LINE

$$n + p \rightarrow d + \gamma$$

$[m_n + m_p] - m_d = 2.223$ MeV (d binding energy)

note: capture on other elements not significant
due to low abundance relative to H
(^{5}He is unstable and returns the neutron)

^{3}He is an important exception!

$$n + {}^3He \rightarrow t + p$$

radiation-less charge-exchange reaction

even though $^3He/H \approx 1 \times 10^{-5}$,

the cross section is large

$$\sigma_{ce,{}^3He} \approx 1.6 \times 10^4 \, (\sigma_{capture,H})$$

2.223 MeV NEUTRON-CAPTURE LINE (cont.)

$$\sigma_{capture} \propto v^{-1}$$

neutrons thermalize in the dense photosphere (T ~ 6000K) before capture

Consequences:

- Line width due to thermal Doppler broadening is very small (<10 eV)
- γ rays are delayed by ~100 s after neutrons are produced
- Significant attenuation of the line due to Compton scattering

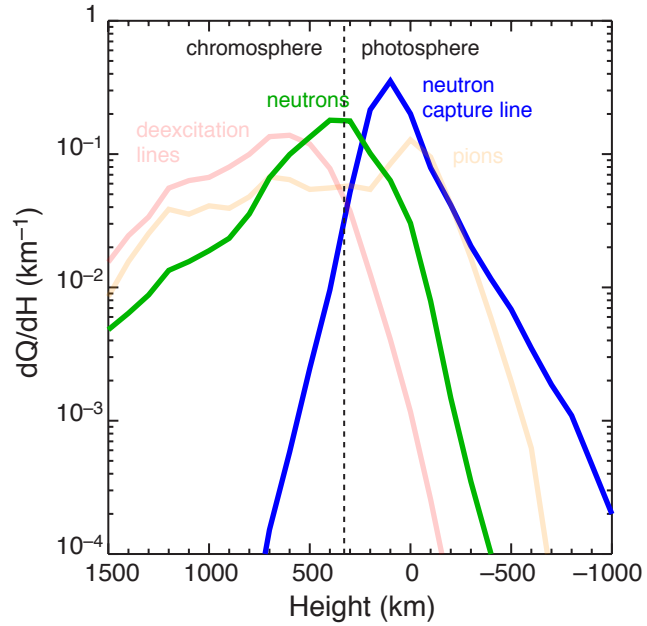

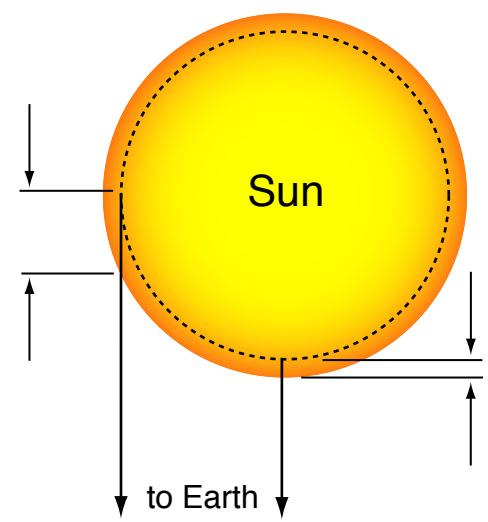

2.223 MeV NEUTRON-CAPTURE LINE (cont.)
Calculated Yields & Ratios

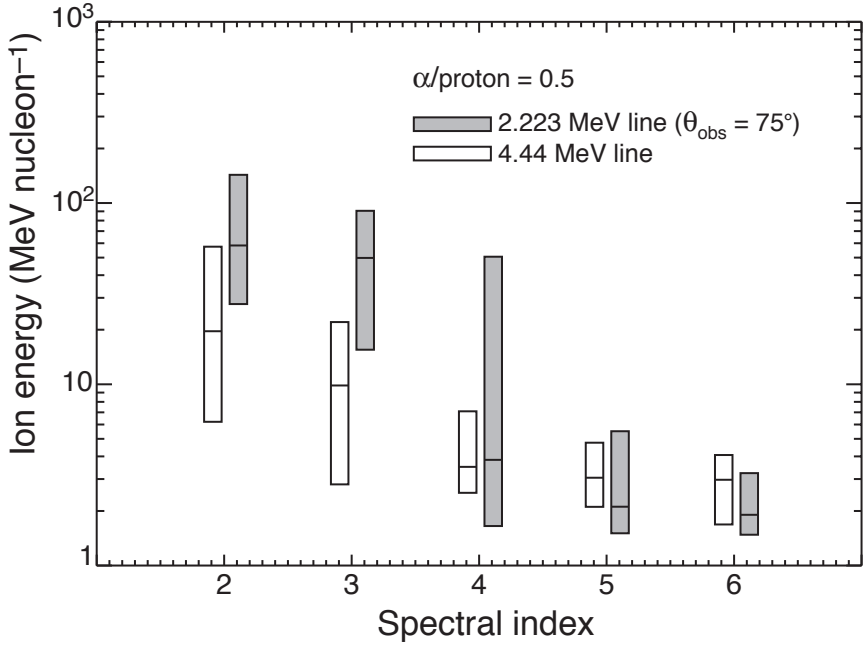

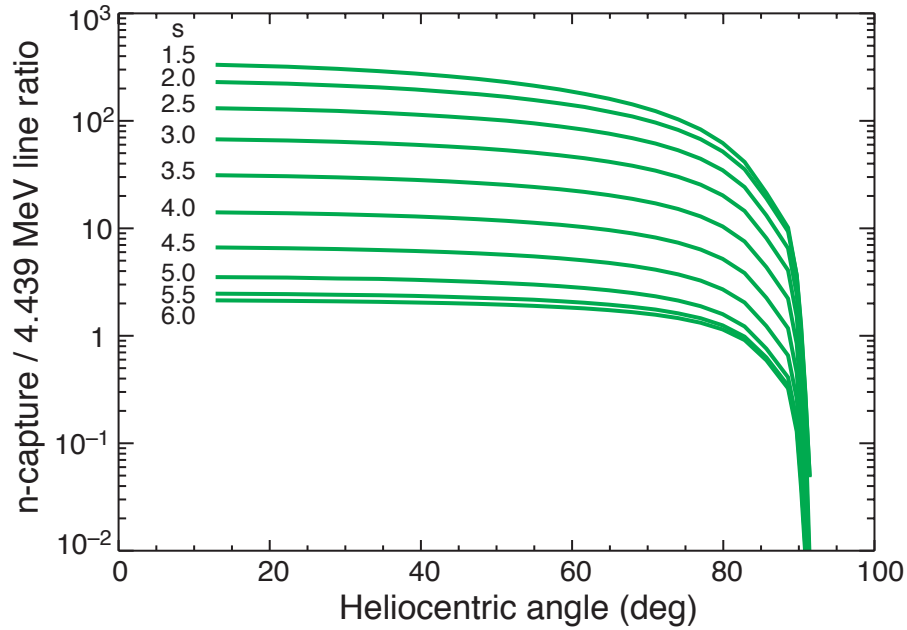

Pion Production

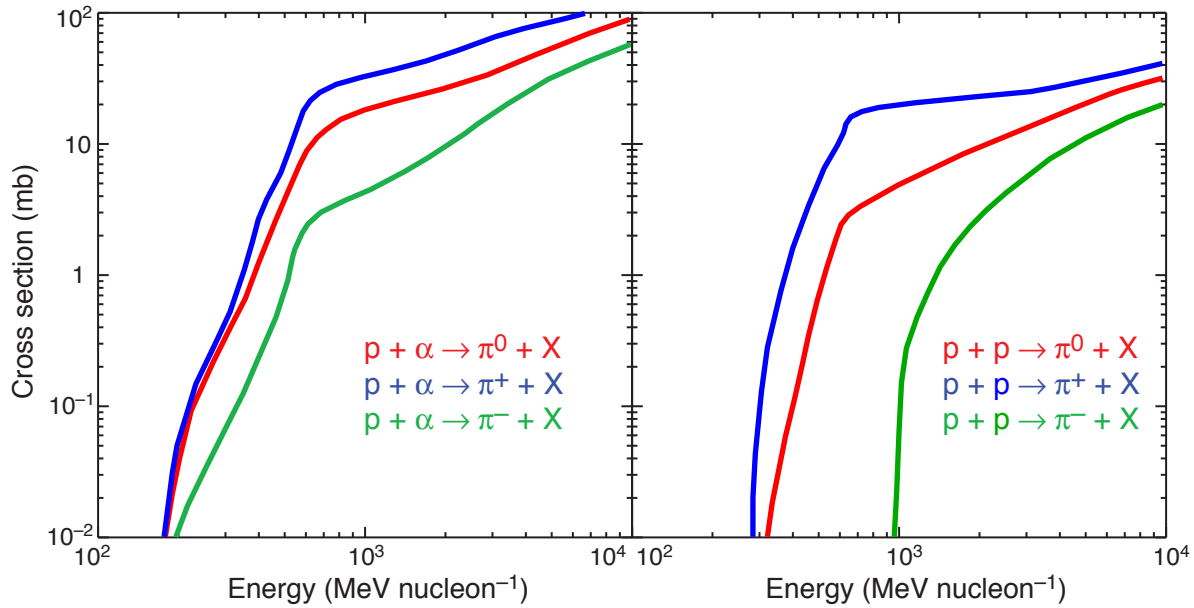

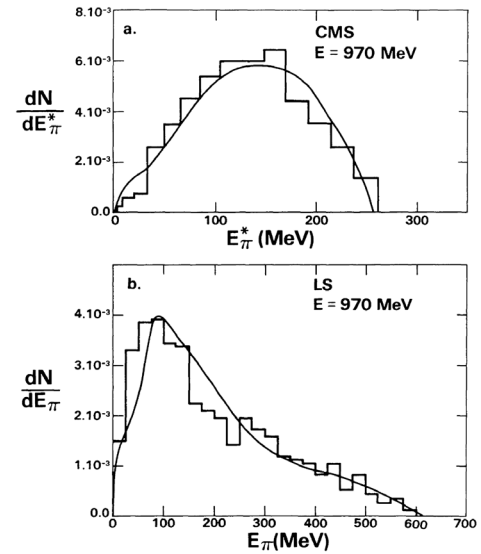

$\pi^0 \rightarrow 2\gamma \quad m_{\pi^0} = 135 \text{ MeV} \rightarrow \varepsilon_\gamma = 67.5 \text{ MeV}$

$\pi^{+,-} \rightarrow e^{+,-} \rightarrow$
- γ_{511} (annihilation, both in-flight and after thermalization)
- continuum emission via bremsstralung from both positrons and electrons

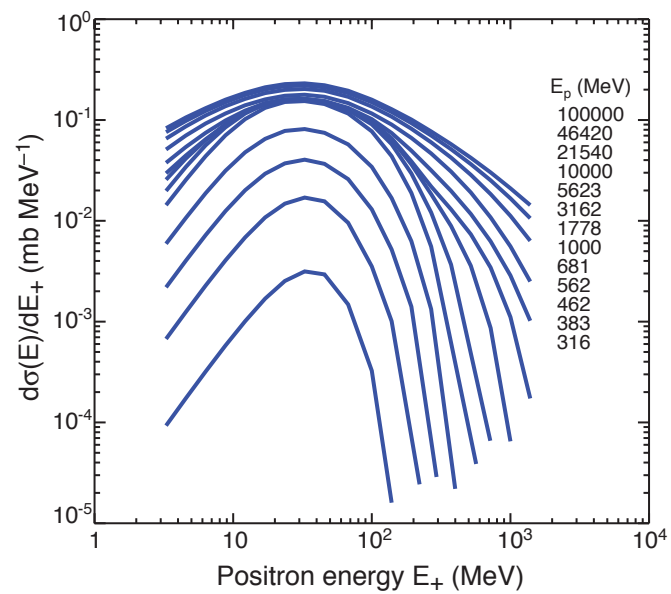

Pion Production (cont.)

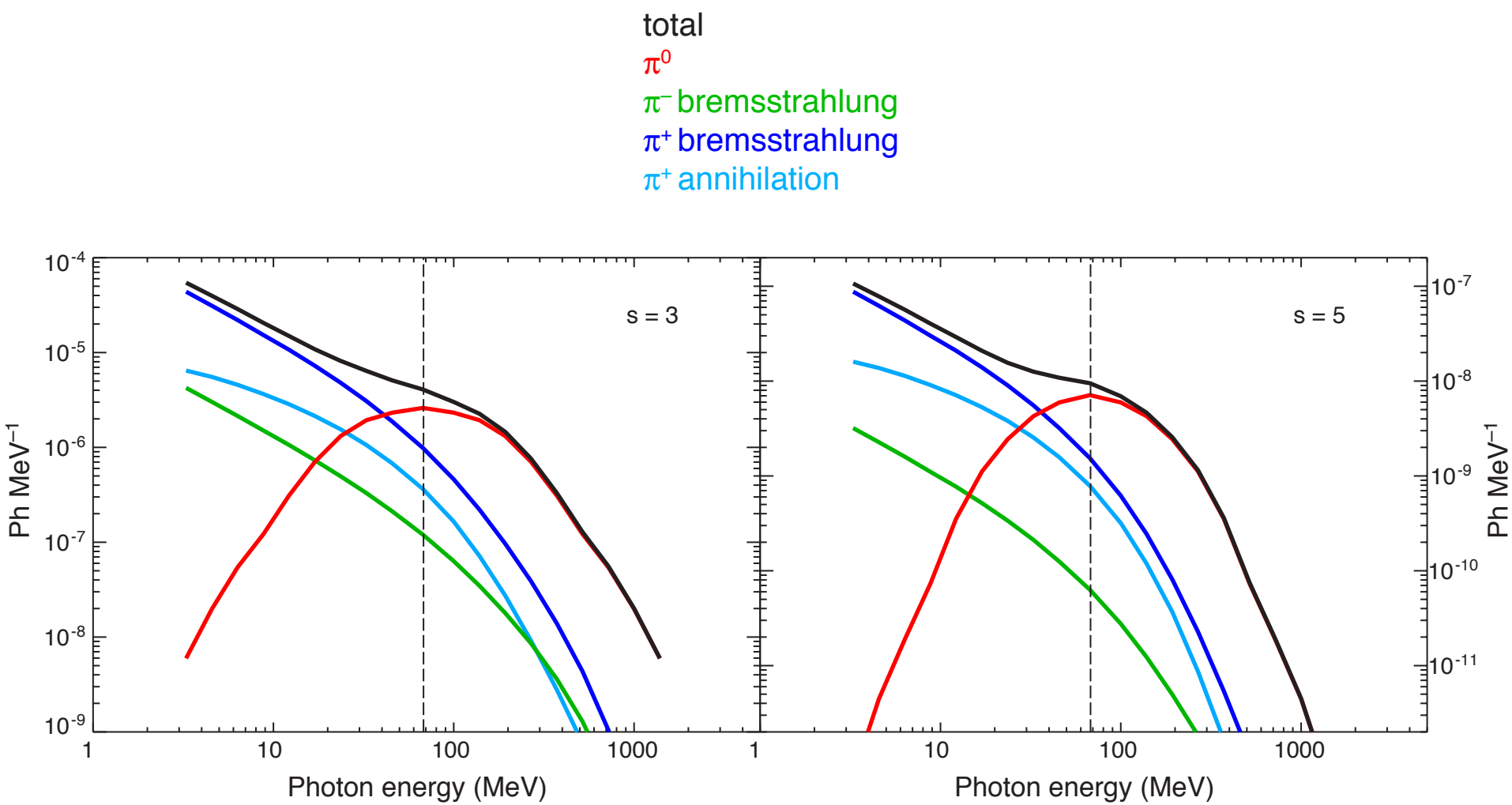

Calculations of High-Energy Observable Emission

The traditional physics approach:

Develop a model for the flare process that can explain the observations with as few physically-based parameters as possible

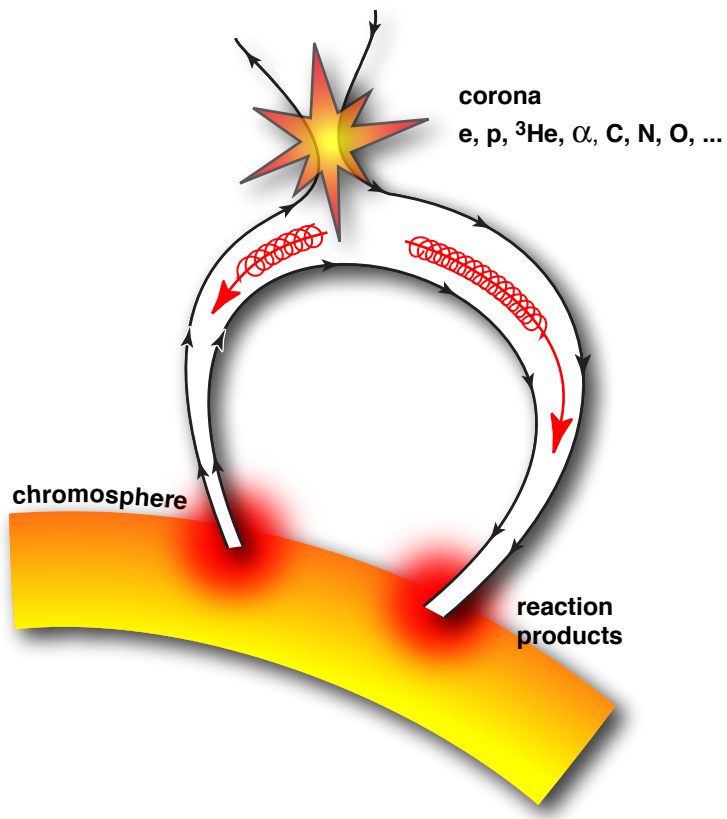

Transport and interaction model described by a set of parameters relating to conditions at the Sun,

$f(p_1, p_2, p_3, \ldots, p_n)$

↓

Predicted observable quantities

↓

Compare with measured observable quantities

↓

Modify parameters $p_1, p_2, p_3, \ldots, p_n$

Magnetic Loop Model

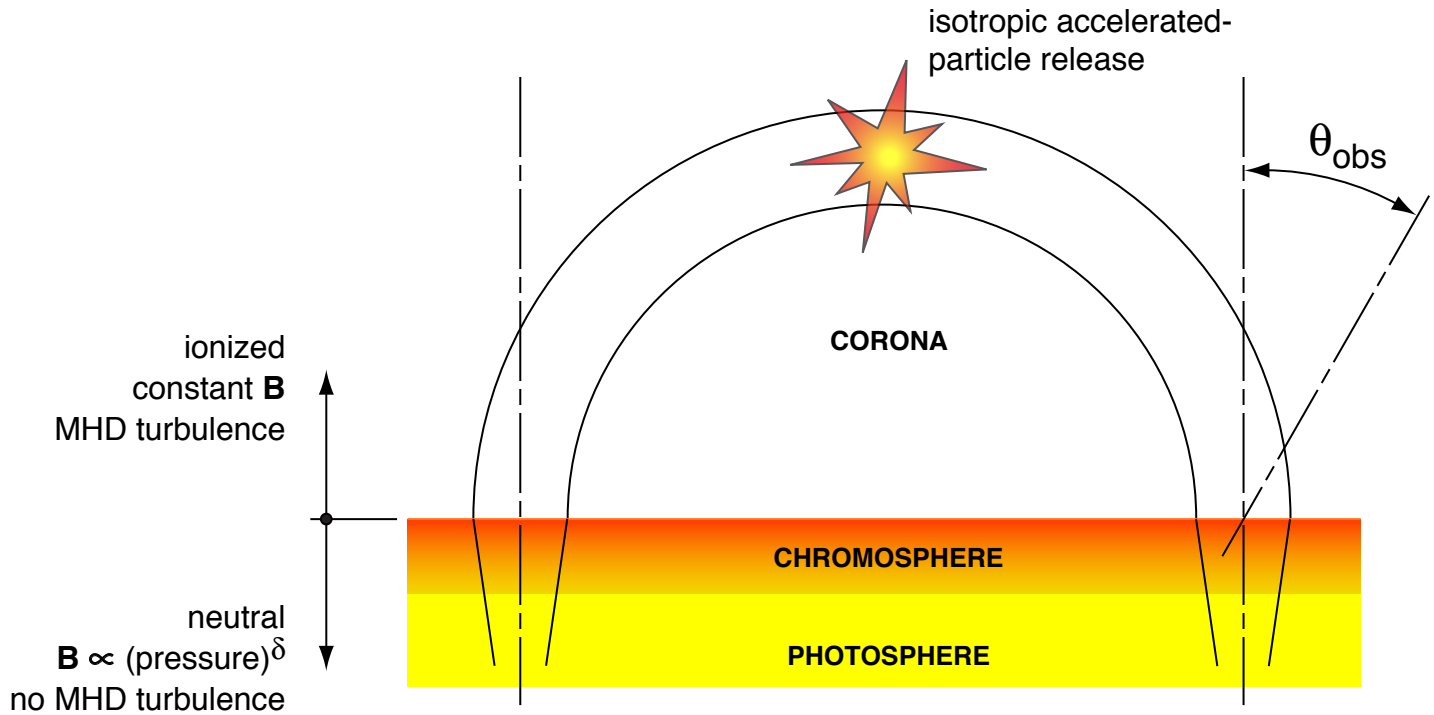

- Scattering due to MHD turbulence replenishes loss cone: $\lambda = \frac{\Lambda}{L_c}$ (mean free path) (loop half length)
- Mirroring due to magnetic field convergence: $B(h) \propto P(h)^{\delta}$
- Atmospheric model, n(h), T(h)
- Accelerated-particle spectral index, abundances
- ambient abundances
- **B** perpendicular to solar surface at footpoints

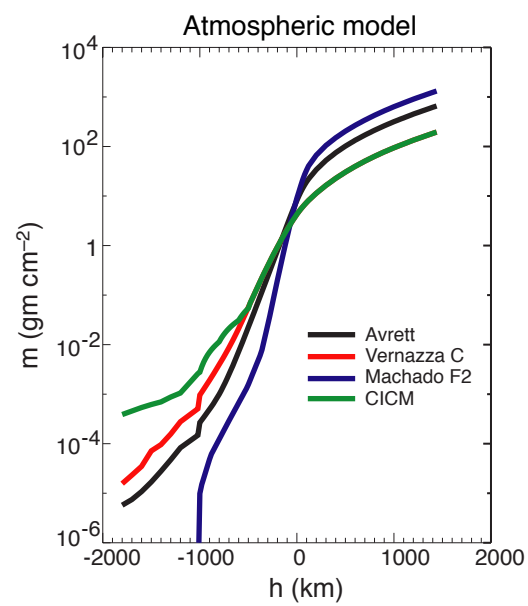

Summary of the Dependence of Observable Quantities on the Parameters

Observable	Acceleration Parameter	Physical Parameter
narrow deexcitation line fluences & ratios	α/p, s	ambient abundances
narrow deexcitation line shift and shape	α/p, s	δ, λ, $\theta_{\rm obs}$, $n(h)$
narrow deexcitation line time history	$a_{\rm ion}(t)$	δ, λ, L_c, $n(h)$
electron bremsstrahlung time history	$a_{\rm e}(t)$	L_c
neutron-capture line fluence	α/p, s	δ, λ, $\theta_{\rm obs}$, $n(h)$, ambient ^{3}He/H
neutron-capture line time history	$a_{\rm ion}(t)$, α/p, s	δ, λ, $\theta_{\rm obs}$, L_c, $n(h)$, ambient ^{3}He/H

Observable	Acceleration Parameter	Physical Parameter
neutron fluence at Earth	α/p, s	δ, λ, $\theta_{\rm obs}$, $n(h)$
neutron arrival time history at Earth	$a_{\rm ion}(t)$, α/p, s	δ, λ, $\theta_{\rm obs}$, L_c, $n(h)$
images	—	L_c, $\theta_{\rm obs}$
511 keV line shape and continuum	α/p,^{3}He/ ^{4}He, s	δ, λ, $\theta_{\rm obs}$, $n(h)$, $T(h)$, $X(h)$
511 keV line time history	$a_{\rm ion}(t)$, α/p,s acc. abundances	δ, λ, $\theta_{\rm obs}$, L_c, $n(h)$, $X(h)$
511 keV line fluence	α/p, s,^{3}He/ ^{4}He acc. abundances	δ, λ, $\theta_{\rm obs}$, $n(h)$, $T(h)$, $X(h)$